Mon. Not. R. Astron. Soc. **339,** 772–792 (2003)

Stellar population gradients in Seyfert 2 galaxies: northern sample

D. Raimann,[1⋆] T. Storchi-Bergmann,[1⋆] R. M. González Delgado,[2⋆]
R. Cid Fernandes,[3⋆] T. Heckman,[4⋆] C. Leitherer[5⋆] and H. Schmitt[6⋆†]

[1]*Universidade Federal do Rio Grande do Sul, IF, CP15051, Porto Alegre 91501-970, RS, Brazil*
[2]*Instituto de Astrofísica Andalucía (CSIC), Apto 3004, 18080, Granada, Spain*
[3]*Departamento de Física, CFM, UFSC, Campus Universitário, Trindade, CP476, Florianópolis 88040-900, SC, Brazil*
[4]*Department of Physics & Astronomy, Johns Hopkins University, 3400 N. Charles St, Baltimore, MD 21218, USA*
[5]*Space Telescope Science Institute, 3700 San Martin Drive, Baltimore, MD 21218, USA*
[6]*National Radio Astronomy Observatory, PO Box 0, Socorro, NM 87801, USA*

Accepted 2002 October 25. Received 2002 October 17; in original form 2002 February 21

ABSTRACT

We use high signal-to-noise ratio long-slit spectra in the λλ3600–4700 range of the 20 brightest northern Seyfert 2 galaxies to study the variation of the stellar population properties as a function of distance from the nucleus. In order to characterize the stellar population and other continuum sources (e.g. featureless continuum, FC) we have measured the equivalent width, *W*, of six absorption features, four continuum colours and their radial variations, and performed spectral population synthesis as a function of distance from the nucleus. About half of the sample has Ca II *K* and *G* band *W* values smaller at the nucleus than at 1 kpc from it, owing to a younger population and/or FC. The stellar population synthesis shows that, while at the nucleus, 75 per cent of the galaxies present contribution >20 per cent of ages ⩽100 Myr and/or of an FC, this proportion decreases to 45 per cent at 3 kpc. In particular, 55 per cent of the galaxies have a contribution >10 per cent of the 3-Myr/FC component (a degenerate component in which one cannot separate what is caused by an FC or by a 3-Myr stellar population) at the nucleus, but only 25 per cent of them have this contribution at 3 kpc. As a reference, the stellar population of 10 non-Seyfert galaxies, spanning the Hubble types of the Seyfert (from S0 to Sc) was also studied. A comparison between the stellar population of the Seyferts and that of the non-Seyferts shows systematic differences: the contribution of ages younger than 1 Gyr is in most cases larger in the Seyfert galaxies than in non-Seyferts, not only at the nucleus but up to 1 kpc from it.

Key words: galaxies: active – galaxies: Seyfert – galaxies: stellar content.

1 INTRODUCTION

The relation between recent star formation and nuclear activity in galaxies has been the subject of a number of recent studies. Cid Fernandes & Terlevich (1995) were the first to argue that the blue continuum in Seyfert 2 galaxies was mostly caused by the contribution of young stars rather than by a scattered featureless continuum (FC), if the hypotheses of unified models for Seyfert galaxies were correct (Antonucci 1993). Heckman et al. (1995) reached similar conclusions using a different method. Heckman et al. (1997) and González Delgado et al. (1998) have proved this to be the case for a few Seyfert 2 galaxies with available ultraviolet (UV) spectra with high enough signal-to-noise ratio to show the wind lines of young O and B stars. González Delgado et al. (1998) have also shown that, in these cases, high-order Balmer lines in absorption, characteristic of young and intermediate-age stars (≈100 Myr), were also present in the spectra. As optical spectra are more easily available, the high-order Balmer lines could thus be used as unambiguous signatures of the presence of young to intermediate-age stars.

In Cid Fernandes, Storchi-Bergmann & Schmitt (1998), Storchi-Bergmann, Cid Fernandes & Schmitt (1998) and Schmitt, Storchi-Bergmann & Cid Fernandes (1999), we used long-slit spectra of approximately 40 active galactic nuclei (AGN) to measure absorption-line and continuum spectral features within a few kiloparsecs from the nucleus, to characterize the stellar population. For the 20 Seyfert 2 galaxies of the sample, we have then performed spectral synthesis of the nuclear spectra, having concluded that the main common characteristic was an excess of an intermediate-age

⋆E-mail: raimann@if.ufrgs.br (DR); thaisa@if.ufrgs.br (TS); rosa@iaa.es (RMGD); cid@fsc.ufsc.br (RCF); heckman@pha.jhu.edu (TH); leitherer@stsci.edu (CL); hschmitt@nrao.edu (HS)
†Jansky Fellow.

stellar population (≈100 Myr) when compared with early-type non-Seyfert galaxies.

Storchi-Bergmann et al. (2000) used stellar population templates to investigate the effect of combining an old bulge population (present in most Seyferts) with a younger one, in particular to investigate the detectability of the high-order Balmer lines as signatures of the young and intermediate-age stars. By comparing the models with the data, we concluded that unambiguous signatures of such stars were present in only 30 per cent of the sample. We have also concluded that is not possible to distinguish a stellar population younger than 10 Myr from a power-law continuum, when these components contribute with less than 40 per cent of the light at 4020 Å.

Combining the above results with the stellar population analysis performed by González Delgado, Heckman & Leitherer (2001) for a northern sample of 20 Seyfert 2 galaxies, we conclude that 40 per cent of nearby Seyfert 2 galaxies present unambiguous signatures of recent episodes of star formation in the nuclear region. In another 30 per cent, a blue component is also necessary to reproduce the near-UV continuum, but its faintness precludes a firm identification, and this component can either be caused by an FC or a stellar population younger than 10 Myr, or both. Joguet et al. (2001), studying the circumnuclear stellar population of the host galaxies of 79 Seyfert 2 nuclei also found high-order Balmer lines seen in absorption in many cases, concluding that young stellar populations are present in around 50 per cent of Seyfert 2 nuclei, a rate similar to that found by us.

In Cid Fernandes et al. (2001b) and Storchi-Bergmann et al. (2001) we have looked for relations between the age of the stellar population in the nuclear region and the host galaxy properties and environment. We have found that the AGNs with largest contributions of recent star formation occur in galaxies with the largest infrared (IR) luminosities; these galaxies are frequently in interactions and present distorted inner morphologies. An evolutionary scenario was suggested, in which the interactions trigger both the nuclear activity and bursts of star formation. The bursts then fade before the nuclear activity, which is thus also found in galaxies with old stellar populations.

In the near-IR, Oliva et al. (1999) studied stellar absorption lines in 13 obscured AGNs and eight genuine Seyfert 1s and found that the presence of powerful starbursts in obscured AGNs is relatively common while they are not present in Seyfert 1s.

In more luminous objects, Aretxaga et al. (2001) found young stellar populations in the nuclear regions of some nearby radio galaxies, and Tadhunter et al. (2002) for intermediate redshift ones. Canalizo & Stockton (2001) studied a sample of low-redshift quasi-stellar objects (QSOs) that may be in a transitionary stage between ultraluminous infrared galaxies (ULIGs) and QSOs and found that every object shows strong recent star-forming activity (younger than 300 Myr) and in many cases this activity is closely related to tidal interactions.

A number of questions are nevertheless still open regarding the hosts of AGNs, and one of a fundamental nature is whether there are any systematic differences between the hosts of AGNs and non-active galaxies of the same Hubble type. In other words: does the onset of nuclear activity relate to large-scale properties of the host galaxies? In the evolutionary scenario described above, for example, if interactions are responsible for triggering the activity and circumnuclear bursts of star formation, would not the more external regions also be affected?

In order to answer the above questions we now extend the study of the stellar population to the extranuclear regions of Seyfert galaxies. As a first step towards this goal, in Raimann et al. (2001, hereafter R01) we have analysed the nuclear and extranuclear stellar population of three early-type (Hubble-type S0) non-Seyfert, two low-ionization nuclear emission-line region galaxies (LINERs) and three Seyfert 2 galaxies as a function of distance from the nucleus. While we found a common behaviour for non-Seyfert galaxies and LINERs, this is not true for the three Seyferts, and a larger sample is needed to characterize the stellar population gradients in Seyferts. We have thus decided to extend this study to the samples of Storchi-Bergmann et al. (2000, called the southern sample) and González Delgado et al. (2001, called the northern sample), which comprise 25 Seyfert 2 galaxies with $z < 0.02$ plus 10 with $0.02 < z < 0.05$. This sample can be considered as representative of nearby Seyfert 2 galaxies. The common selection criterion for all the galaxies is a lower limit for the luminosity of the central source, such that the luminosity in the [O III] λ5007 line is $L_{[\mathrm{O\,III}]} > 10^{40}$ erg s^{-1}. As it was not selected by any property related to the stellar population, it is suitable for exploring this property.

As the spectra of the northern and southern samples cover distinct wavelength ranges, we have performed the two studies separately. In this work we analyse the northern sample and in a future work the southern one. We first quantify the radial variations of the equivalent widths and continuum fluxes as a function of the distance from the nucleus, used to measure the dilution of the bulge absorption lines by an FC or a young stellar population at the nucleus. Then we use these measurements to perform a spectral synthesis and to derive the stellar population properties and gradients.

This paper is organized as follows. In Section 2 we describe the sample galaxies and the observations. In Section 3 we discuss the spatial variation of the equivalent widths and continuum. We present the spectral synthesis results in Section 4 and, in Section 5, the discussion and in Section 6 the conclusions of this work.

2 SAMPLE AND OBSERVATIONS

Detailed information concerning the observations and reductions of the long-slit spectra of the northern sample can be found in González Delgado et al. (2001). It comprises the brightest 20 Seyfert 2 galaxies from the compilation of Whittle (1992a,b). The radial velocities range from 1000 to 15 000 km s^{-1} but only five objects have radial velocities >9000 km s^{-1}. The value mean is 4811 km s^{-1}, which gives a mean spatial scale of 310 pc arcsec^{-1}. In Table 1 we list the morphological type, radial velocity, spatial scale (using $H_0 =$ 75 km s^{-1} Mpc^{-1}) and foreground galactic $E(B-V)_G$ values. The data were extracted from the NASA/IPAC Extragalactic Data base (NED).[1]

Long-slit spectra of these galaxies have been obtained using the Richey–Chrétien spectrograph at the 4-m Mayall telescope of Kitt Peak National Observatory in 1996 February and October. The long-slit spectra used in this work cover the wavelength range 3600–4700 Å, at a resolution of ≈3 Å. Each pixel at the detector corresponds to 0.7 arcsec on the sky. A slit width corresponding to 1.5 arcsec on the sky was oriented along the parallactic angle except for NGC 1068 on which it was oriented at PA = 123°. For two galaxies, NGC 5929 and Mrk 477, we have two position angles, PA = 60°, 80° and PA = 44°,158°, respectively.

One-dimensional spectra were extracted in windows of 2.1 arcsec in the bright nuclear regions and progressively larger windows towards the fainter outer regions. The spectra were dereddened

[1] The NASA/IPAC Extragalactic Data base is operated by the Jet Propulsion Laboratory, California Institute of Technology, under contract with the National Aeronautics and Space Administration.

Table 1. The Seyfert 2 galaxies sample.

Name	Type	v (km s^{-1})	1 arcsec (pc)	$E(B-V)_G$
Mrk 1	S	4780	310	0.060
Mrk 3	S0	4050	260	0.188
Mrk 34	S	15 150	980	0.009
Mrk 78	SB	11 145	720	0.035
Mrk 273	Ring. Gal pec	11 334	730	0.008
Mrk 348	SA(s)0/a	4540	290	0.067
Mrk 463E	S pec	14 904	960	0.030
Mrk 477	S	11 340	730	0.011
Mrk 533	SA(r)bc pec	8713	563	0.059
Mrk 573	SAB(rs)0+	5174	335	0.023
Mrk 1066	SB(s)0+	3605	235	0.132
Mrk 1073	SB(s)b	6991	450	0.160
NGC 1068	SA(rs)b	1136	75	0.034
NGC 1386	SB(s)0+	924	60	0.012
NGC 2110	SAB0-	2284	150	0.375
NGC 5135	SBab	4112	270	0.060
NGC 5929	Sab:pec	2753	180	0.024
NGC 7130	Sa pec	4842	310	0.029
NGC 7212	S	7994	515	0.072
IC3639	SBbc	3285	210	0.069

Table 2. The non-Seyfert galaxies sample.

Name	Type	v (km s^{-1})	1 arcsec (pc)	$E(B-V)_G$
NGC 1232	SAB(rs)c	1500	97	0.026
NGC 1367	(R′)SAB(r′l)a	1500	97	0.024
NGC 1425	SA(rs)b	1500	97	0.013
NGC 1637	SAB(rs)c	600	39	0.040
NGC 3054	SAB(r)bc	2400	155	0.074
NGC 3223	SA(r)bc	3000	194	0.108
NGC 3358	(R′2)SAB(l)ab	3000	194	0.055
NGC 7049[a]	SA(s)0	2231	116	0.007

[a]Observed by Raimann et al. (2001).

according to foreground galactic $E(B-V)_G$. The spatial coverage ranged between 3 (for Mrk 34) and 50 arcsec (NGC 1068) from the nucleus. The signal-to-noise (S/N) ratio of the extracted spectra ranges between 10 and 40.

In order to compare the stellar population of these active galaxies with that of non-active ones of the same Hubble type, we have also obtained long-slit spectra of nearby non-Seyfert galaxies with morphological types between Sa and Sc. We used the R-C Cassegrain Spectrograph at the 1.5-m telescope of Cerro Tololo Inter-American Observatory during 2002 January (Table 2). Owing to the proximity of these galaxies, the nuclear spectrum was extracted in a window of 3 arcsec, in order to allow a similar sampling at the galaxy to that of the Seyferts. Extranuclear spectra were extracted up to approximately 8 arcsec from the nucleus. The spectra were dereddened according to foreground galactic $E(B-V)_G$. In addition, to represent the S0 Hubble type, we use the data from the S0 non-Seyfert galaxy NGC 7049 (see the bottom of Table 2), already presented in R01, which is representative of the three S0 galaxies studied in that paper.

Because the number of non-Seyfert galaxies is still small, we use as an additional reference the study of Bica (1988, hereafter B88), in which he performed stellar population synthesis for approximately 100 non-Seyfert galaxies, using integrated spectra from regions of approximately 1×1 kpc^2. B88 grouped the galaxies spectra into six templates, called S1–S6. Templates S1 and S2 are dominated by galaxies with Hubble types Sa, templates S3 and S4 by Sbs and templates S5 and S6 by Scs.

3 RADIAL VARIATION OF THE EQUIVALENT WIDTHS AND CONTINUUM COLOURS

The variation of the equivalent widths (Ws) of absorption lines and the continuum colours as a function of distance from the nucleus allows the study of stellar population gradients in the galaxy. Usually, in non-active galaxies, the Ws increase from the external regions towards the bulge, where they remain approximately constant. The presence of a burst of star formation and/or a featureless AGN continuum will produce a 'dilution' of the absorption lines, the Ws of which will then decrease at the nucleus when compared with the values at adjacent locations (Cid Fernandes et al. 1998).

In order to study the run of the stellar absorption features with distance from the nucleus we determined a pseudo-continuum at selected pivot points and measured the Ws of six absorption features as described in R01. Owing to the shorter spectral range of the present work the pivot points used here for the continuum were 3660, 3780, 4020 and 4510 Å and the absorption features for which we measured the Ws were: $W_{\rm wlb}$ (a blend of weak lines in the near-UV, within the spectral window λλ3810–3822), H9 (a blend of absorption lines that includes H9, λλ3822–3858), Ca II K (λλ3908–3952), Ca II H+Hϵ (λλ3952–3988), *CN* band (λλ4150–4214) and *G* band (λλ4284–4318).

In Figs 1–3 we present the above Ws, continuum colour F_{4510}/F_{4020} (hereafter $C_{4510/4020}$) and surface brightness as a function of the angular distance from the nucleus for the Seyfert 2 galaxy sample. The typical errors are 0.5 Å for $W_{\rm wlb}$, H9, Ca II K, Ca II H+Hϵ and *G* band, 1.0 Å for the *CN* band and 0.05 for the continuum ratio (Cid Fernandes et al. 1998). The dotted and dashed vertical lines mark distances at each galaxy of 1 and 3 kpc from the nucleus, respectively. The measurements for Mrk 463 are not presented here because these data are already shown in R01. We also do not show the data for Mrk 78 because it has only one extranuclear spectrum to each side. We present data for just one position angle of Mrk 477 and NGC 5929 because the other PAs show similar behaviours. Measurements of Ca II *K* and *G* band Ws for some of these objects were showed in González Delgado et al. (2001) but they are different from those showed here owing to a different pseudo-continuum adopted. As five galaxies of the present sample are also in the sample of Cid Fernandes et al. (1998), we can compare our measurements with theirs in order to check the robustness of the method. We point out that the measurements in the above paper were obtained with a different instrument and along different position angles, although using the same technique. Nevertheless, a careful comparison shows that the W values for the same feature are remarkably similar, usually within the measurement errors.

In Fig. 4 we show the same quantities for the non-Seyfert S0 galaxy NGC 7049, first presented in R01. For the non-Seyfert Sa–Sc galaxies, it was only possible to obtain signal-to-noise ratios high enough for reliable measurements for the nucleus and usually a couple of extractions to each side of the nucleus. The corresponding values are summarized below.

The range of nuclear Ws obtained for Seyfert 2 galaxies is $0 < W_{\rm wlb} < 3.5$, $0 < W_{\rm H9} < 11$, $2 < W_{\rm Ca\,II\,K} < 15.5$, $0 < W_{\rm Ca\,II\,H+H\epsilon} < 9$, $2.5 < W_{\rm CN\,band} < 14$ and $1 < W_{G\,\rm band} < 9.5$ Å. While the nuclear values for the S0 are $W_{\rm wlb} \approx 6$, $W_{\rm H9} \approx 20$, $18 < W_{\rm Ca\,II\,K} < 20$, $12 < W_{\rm Ca\,II\,H+H\epsilon} < 14$, $17 < W_{\rm CN\,band} < 19$ and $W_{G\,\rm band} \approx 11$ Å, those of the Sa–Sc are $1 < W_{\rm wlb} < 4$, $6 < W_{\rm H9} < 15$, $7 < W_{\rm Ca\,II\,K} < 18$, $8 < W_{\rm Ca\,II\,H+H\epsilon} < 13$, $3 < W_{\rm CN\,band} < 13$ and 4

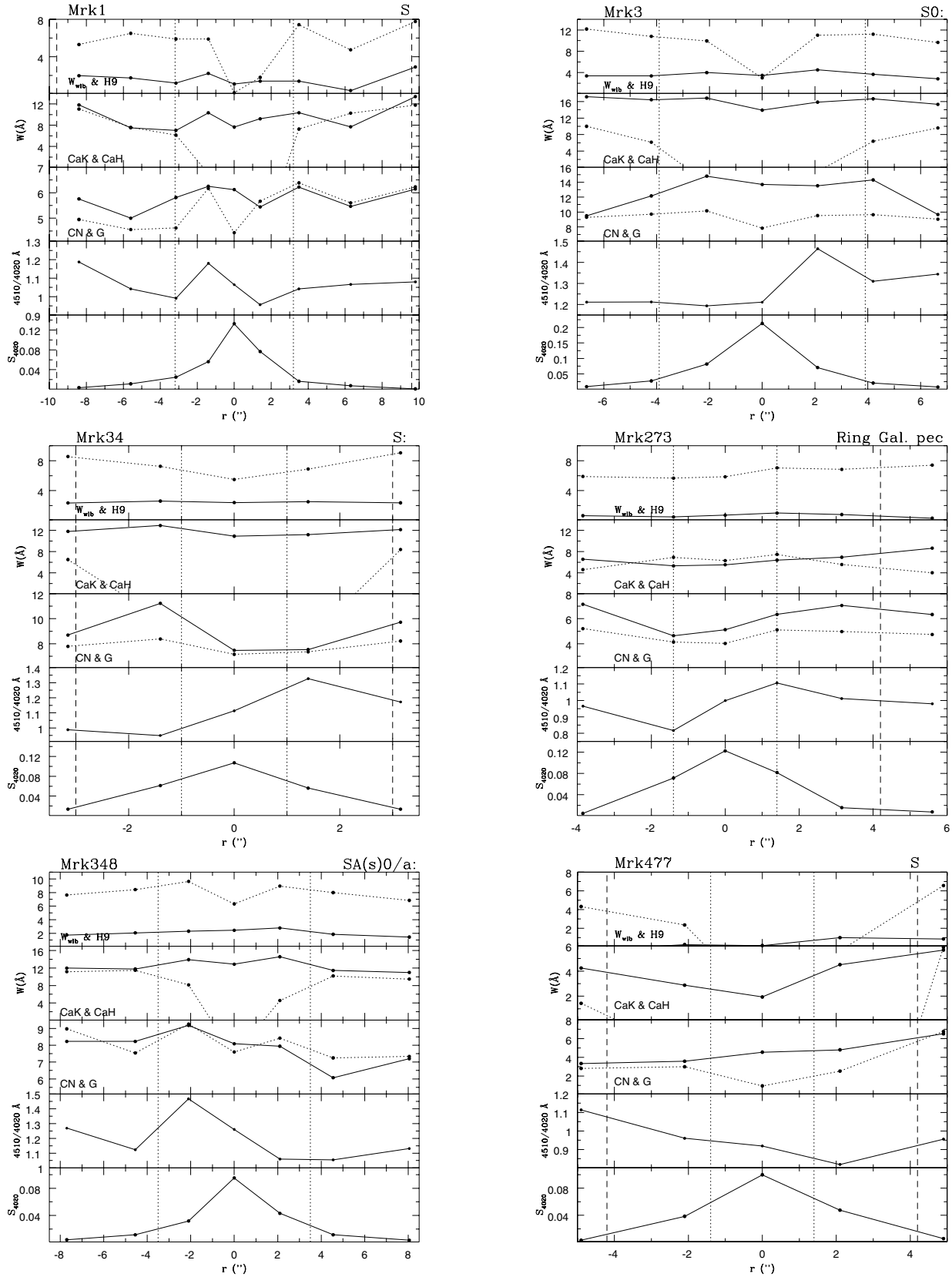

Figure 1. Seyfert 2 galaxies: radial variations of the equivalent widths, continuum colour and surface brightness. The first panel shows $W_{\rm wlb}$ (solid line) and $W_{\rm H9}$ (dotted), the second shows $W_{\rm Ca\,II\,K}$ (solid) and $W_{\rm Ca\,II\,H+H\epsilon}$ (dotted), the third, $W_{\rm CN\,band}$ (solid) and $W_{G\rm band}$ (dotted). The fourth panel shows the continuum colour $C_{4510/4020}$. The fifth panel shows the run of the surface brightness at 4020 Å (in units of 10^{-15} erg cm^{-2} s^{-1} Å^{-1} arcsec^{-2}) along the slit. The dotted and dashed vertical lines mark distances of 1 and 3 kpc from the nucleus, respectively.

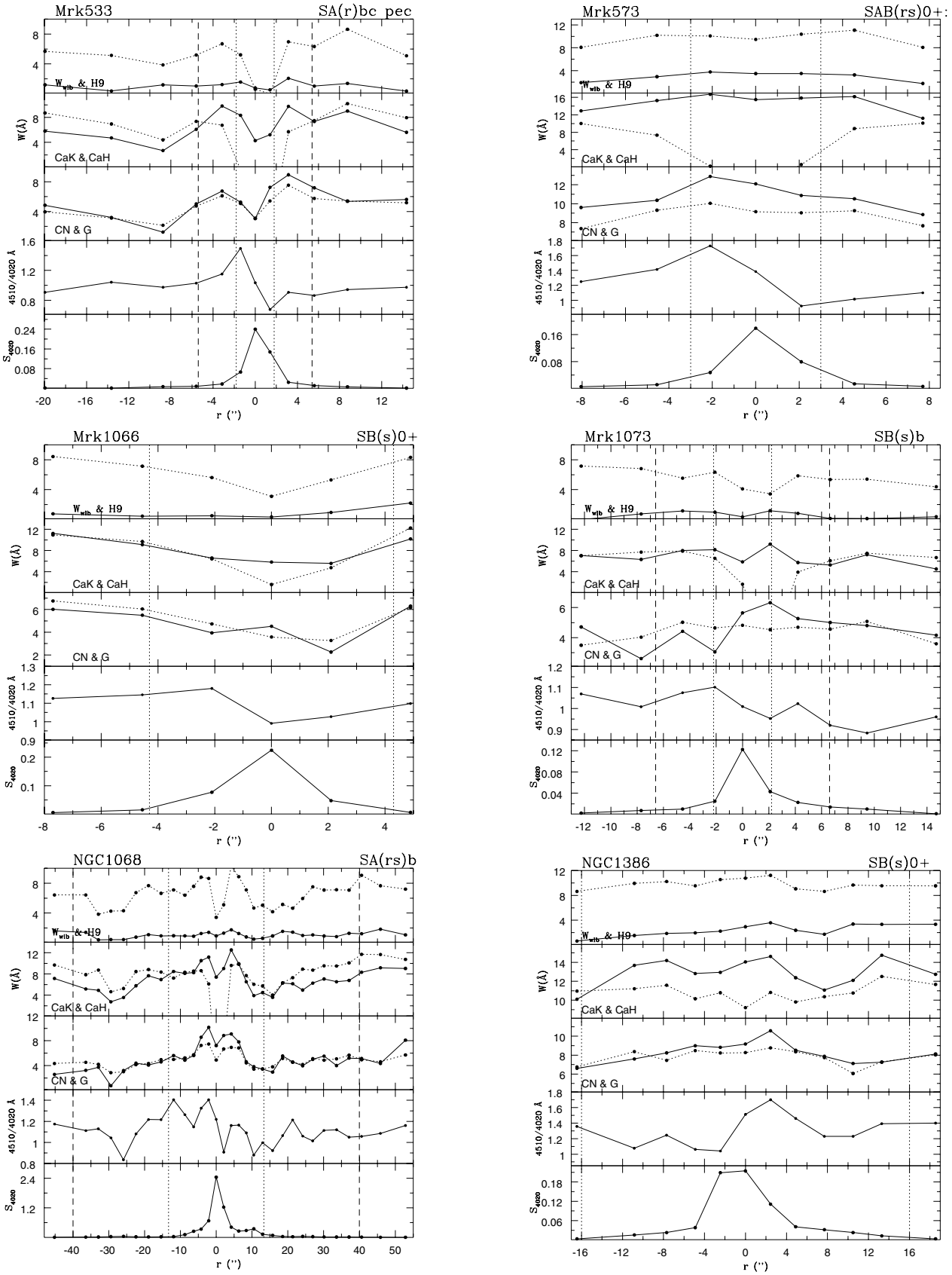

Figure 2. Seyfert 2 galaxies: radial variations of the equivalent widths, continuum colour and surface brightness. The symbols are as in Fig. 1.

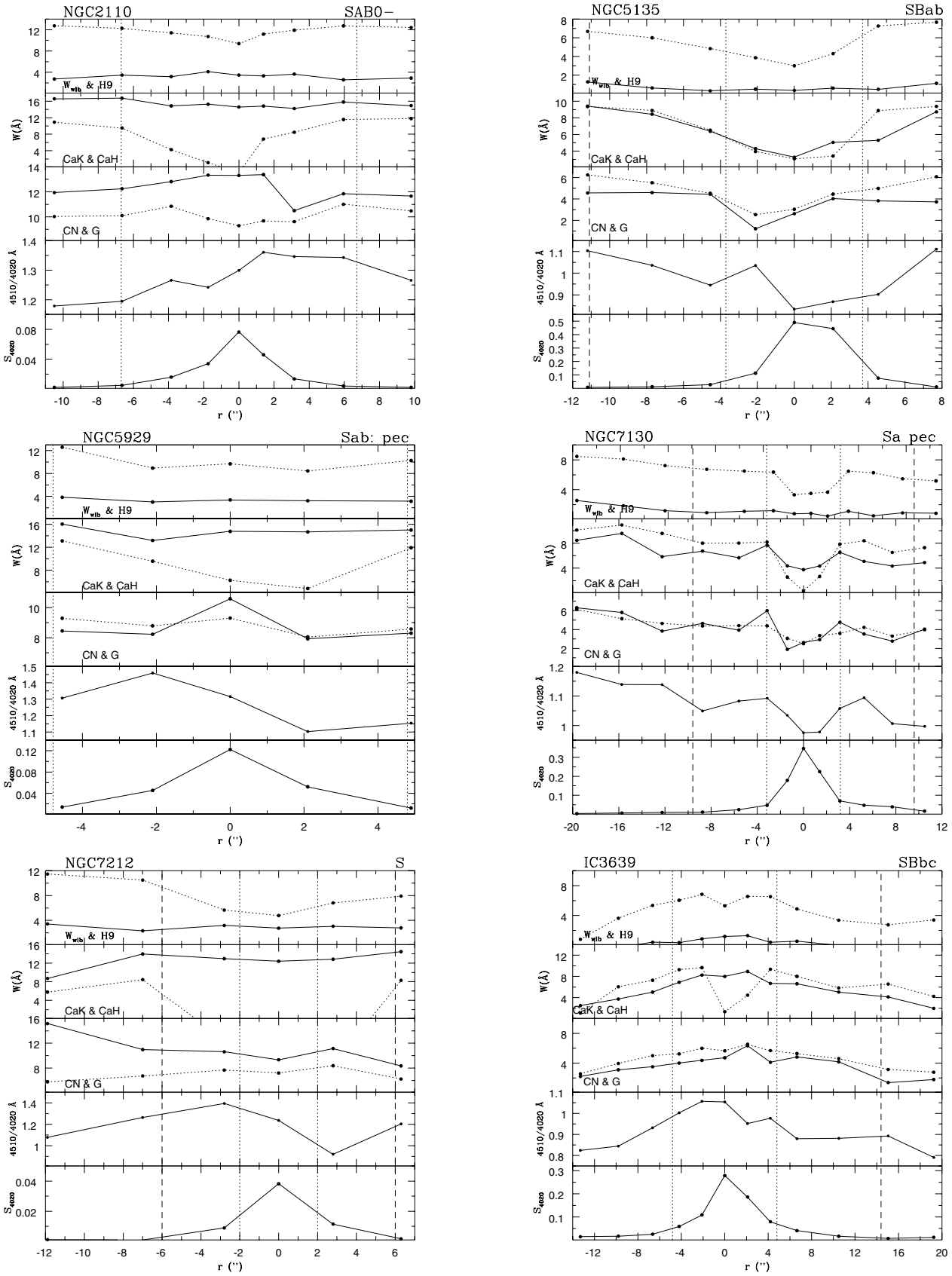

Figure 3. Seyfert 2 galaxies: radial variations of the equivalent widths, continuum colour and surface brightness. The symbols are as in Fig. 1.

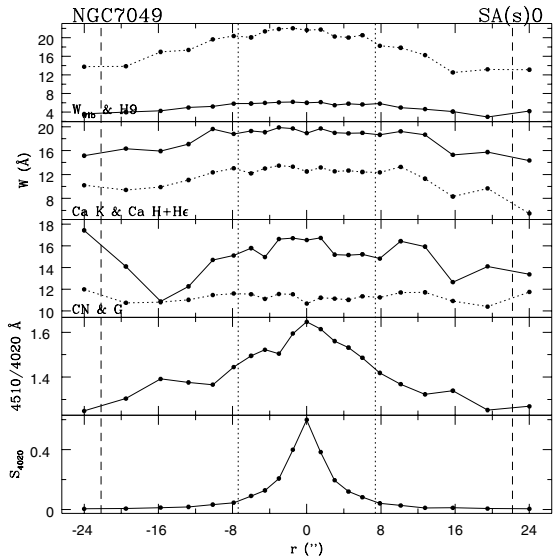

Figure 4. Non-Seyfert S0 galaxy NGC 7049: radial variations of the equivalent widths, continuum colour and surface brightness. The symbols are as in Fig. 1.

$< W_{G\,\mathrm{band}} < 10$ Å. The non-Seyfert Sa–Sc galaxies thus present nuclear *W* values considerably smaller than that of the non-Seyfert S0, but the radial variations show a similar trend.

Almost all Seyfert 2s have some gas emission in the nuclear lines H9 and Ca II H+Hϵ, and sometimes this emission is present in the extranuclear spectra too. Mrk 463E and Mrk 477 are examples of objects dominated by extended gas emission. Therefore, almost all Seyfert 2 galaxies have these lines with smaller *W*s in and near the nucleus.

In non-Seyfert S0 galaxies most *W*s have the largest values at the nucleus, decreasing outwards (e.g. Fig. 4). Two Seyferts, Mrk 348 and IC3639, present a similar trend, with *W*s increasing towards the nucleus, although at the nucleus proper they show a sudden decrease. If we focus our attention in the behaviour of $W_{\mathrm{Ca\,II\,K}}$ and *G* band, the lines with the smallest measurement errors, we realize that approximately half the sample (galaxies listed in Table 3) have these nuclear *W*s smaller than the extranuclear ones. This behaviour is probably caused by dilution of the bulge stellar population by a blue continuum that can either be caused by an FC component or a young stellar population, or both.

Table 3. Dilution percentage of the nuclear Ca II *K* and *G* band in relation to 1 kpc from the nucleus.

Name	$f(\lambda)$ (per cent) Ca II K	*G* band
Mrk 1	13 ± 13	17 ± 13
Mrk 3	10 ± 6	18 ± 1
Mrk 463E	55 ± 6	70 ± 4
Mrk 477	45 ± 12	66 ± 2
Mrk 533	55 ± 1	54 ± 5
Mrk 1066	40 ± 3	41 ± 1
NGC 1068[a]	35 ± 6	30 ± 2
NGC 2110	5 ± 3	12 ± 4
NGC 5135	44 ± 6	36 ± 3
NGC 7130	46 ± 4	36 ± 6
NGC 7212	3 ± 1	10 ± 4

[a]Relative to 5 arcsec (375 pc) from the nucleus.

We estimate the fraction of the continuum associated with the above blue component $f(\lambda)$ at the wavelength of an absorption line as

$$f(\lambda) = \frac{W_{\text{off-nuc}} - W_{\text{nuc}}}{W_{\text{off-nuc}}}, \quad (1)$$

where W_{nuc} and $W_{\text{off-nuc}}$ are the *W*s at the nucleus and outside, respectively (Cid Fernandes et al. 1998).

In Table 3 we show the dilutions $f(\lambda)$ of the nuclear Ca II *K* and *G* band. These dilutions are measurements of the contribution of an FC or a younger population at the nucleus, as compared with that at 1 kpc. The uncertainties listed in the table are measurements of the difference between the dilution factors obtained using the two extranuclear extractions at opposite sides of the nucleus. In the remaining Seyferts there is no obvious dilution, nor a systematic variation with the distance similar to that observed for the S0 galaxy.

Regarding the continuum, two galaxies (Mrk 78 and IC3639) have the nuclear $C_{4510/4020}$ redder than the extranuclear ones similarly to those of the non-Seyfert early-type galaxies. Four others have the nuclear continuum bluer than that of the extranuclear region (Mrk 1066, Mrk 477, NGC 5135 and NGC 7130) and in the remainder (14 galaxies) the $C_{4510/4020}$ behaviour is not symmetrical relative to the nucleus. This is likely to be caused by a non-uniform dust distribution, in agreement with *Hubble Space Telescope* (*HST*) images of the inner region of these galaxies, many of which were published by Malkan, Gorjian & Tam (1998, their fig. 2).

3.1 NGC 1068

NGC 1068 is considered the prototypical Seyfert 2 and it is the brightest galaxy of the sample, allowing a more detailed study of its stellar population, as high signal-to-noise ratio spectra could be extracted up to ≈50 arcsec (3.7 kpc) from the nucleus, at a spatial sampling of ≈200 pc.

Neff et al. (1994) showed that this galaxy contains multiple components at UV wavelengths: the central AGN, a population of very luminous starburst knots, a bright oval inner disc and a fainter, more circular halo. The knots are mostly located in two star formation rings. One at 10 arcsec from the nucleus (750 pc at the galaxy) – the nuclear ring – that includes the most luminous knot and the other at 28 arcsec from the nucleus (2.1 kpc) – the inner ring – that includes several luminous knots. Our slit was oriented to cover one luminous knot from each ring, labelled regions C and J by Neff and collaborators.

In Fig. 2 (bottom left-hand panel) we show the *W*s, $C_{4510/4020}$ and surface brightness as a function of the angular distance from the nucleus for NGC 1068. All *W*s show a dip at the nucleus relative to the extranuclear values at ≈5 arcsec, where the *W*s reach the largest values (which are, however, still smaller than those of the non-Seyfert early-type galaxy at a similar location). Beyond 5 arcsec, the *W*s decrease, consistent with the presence of star-forming regions along the slit. In particular, at 10 arcsec NW on the nuclear ring, where knot J is located, the *W*s decrease to values smaller than those at the nucleus, while to the other side of the ring the *W*s are similar to the nuclear ones, suggesting that the stellar population is not as young as in knot J. At the inner ring, the smallest *W*s occur at ≈28 arcsec SE, the location of knot C, and are similar to those of knot J, indicating that at the knots there are younger star-forming regions than at other locations along the ring.

The continuum ratio $C_{4510/4020}$ shows a behaviour consistent with that of the *W*s, being bluest close to the regions where the *W*s are

smallest, except for the nucleus, which has a continuum redder than that at 2 arcsec NW but bluer than that at 2 arcsec SE.

In order to calculate the dilution of the *W*s at the nucleus, we have compared the nuclear *W*s with those from the region at 5 arcsec (375 pc at the galaxy) instead of using 1 kpc, because of the nuclear ring at this latter location. All nuclear *W*s are diluted relative to the extranuclear values. H9 and Ca II H+Hϵ are contaminated by gas emission, while Ca II *K* and the *G* band are diluted by approximately 30 per cent. This value is consistent with the known contribution of an FC component (Antonucci, Hurt & Miller 1994).

4 THE SPECTRAL SYNTHESIS

The spectral synthesis was performed using the probabilistic formalism described in Cid Fernandes et al. (2001a). We reproduce the observed *W*s and continuum ratios (*C*s) using a base of star cluster spectra with different ages and metallicities (Bica & Alloin 1986). We use 12 components representing the age–metallicity plane plus a 13th component representing a canonical AGN continuum $F_\nu \propto \nu^{-3/2}$ (Schmitt et al. 1999).

To synthesize the data of this work we have used the *C*s λ3660/4020 and λ4510/4020, and the *W*s $W_{\rm wlb}$, $W_{\rm H9}$, $W_{\rm Ca\,II\,K}$, $W_{\rm CN\,band}$ and $W_{G\,\rm band}$. The adopted errors were $\sigma(W_\lambda) = 0.5$ Å for $W_{\rm wlb}$, $W_{\rm H9}$, $W_{\rm Ca\,II\,K}$ and $W_{G\,\rm band}$, 1.0 Å for $W_{\rm CN\,band}$ and $\sigma(C_\lambda) = 0.05$ for continuum ratios (Cid Fernandes et al. 1998). In some cases the synthesis was performed with a smaller number of *W*s, owing to the contamination by emission lines.

It is important to bear in mind that in this spectral range it is not possible to discriminate between the FC and 3-Myr components for flux contributions smaller than 40 per cent at 4020 Å, because they have very similar continua (Storchi-Bergmann et al. 2000). Therefore, in the description and discussion of the synthesis results we combine the 3-Myr and FC components in one, the 3-Myr/FC component.

According to Cid Fernandes et al. (2001a), this method of spectral synthesis also has difficulty in accurately determining the contributions of all 12 components of Bica's base for a modest signal-to-noise ratio and/or a reduced number of observables. These constraints act primarily in the sense of spreading a strong contribution in one component preferentially among base elements of the same age. Thus, in order to produce more robust results we have grouped components of the same age.

Owing to the fact that the spectral resolution of Bica & Alloin's (1986) templates is lower than that of the present galaxy spectra we need to estimate the effect of this difference in the equivalent width measurements, and in the synthesis results. The equivalent widths are weaker in the lower-resolution case. Therefore, when we use a base with lower resolution than the data, the contribution of the older and/or more metallic populations are overestimated and the contribution of younger and/or less metallic ones are underestimated. These effects are nevertheless small in our sample, as explained below.

Smoothing a few spectra down to the resolution of Bica & Alloin's templates, we have estimated that the differences in the equivalent widths are, in most cases, within the measurement errors (see above). Performing the synthesis with the smoothed spectra, we realized that, on average, the percentage contribution to the light at 4020 Å of the oldest components 10 or 1 Gyr becomes 5 per cent smaller, while the contribution of the youngest component 3-Myr/FC becomes 5 per cent larger, while $E(B-V)$ becomes on average 0.06 larger. These differences do not affect the conclusions of our work, as can be seen in the following sections, and we thus have opted for keeping the full resolution of our data in the synthesis.

4.1 Synthesis results for the non-Seyfert galaxies

In order to compare our results with those for non-Seyfert galaxies we again performed the spectral synthesis for the non-Seyfert galaxy NGC 7049, with the new input parameters specified above in order to verify whether there is any change relative to the results found in R01. There are no significant differences: the stellar population is dominated by the 10-Gyr metal-rich component at the nucleus, with its contribution decreasing beyond 1 kpc, while the contribution of the 1-Gyr component increases outwards. In Fig. 5 we show the synthesis results for this galaxy. The results are presented as proportions of the flux contributed by each component at λ4020 and the internal reddening $E(B-V)_i$ of the galaxy. The panels show from bottom to top the contribution from: the sum of the four 10-Gyr components; the sum of the three 1-Gyr components; the sum of two 100-Myr components; the sum of the two 10-Myr components; the sum of the 3-Myr component and FC ($F_\nu \propto \nu^{-3/2}$). The top panel shows the internal reddening $E(B-V)_i$ obtained from the synthesis. At the bottom panel we also show separately, with open symbols, the sum of the two metal-poor components. The vertical bars are the standard deviation of the results. The vertical lines crossing all panels mark distances of 1 and 3 kpc from the nucleus.

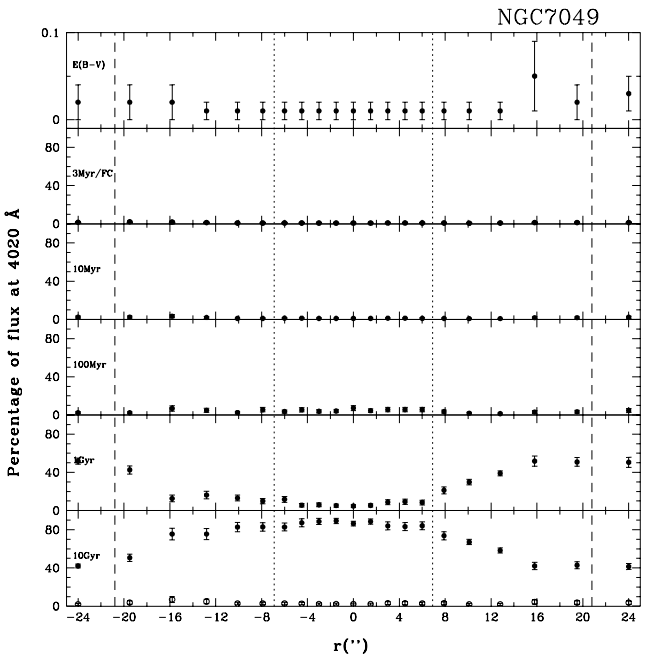

Figure 5. Results of stellar population synthesis using a base of star clusters plus a power-law component $F_\nu \propto \nu^{-3/2}$ for the non-Seyfert galaxy NGC 7049. The dots represent the percentage contribution to the flux at 4020 Å from different age and metallicity components as a function of distance from the nucleus. The panels show from bottom to top, the contribution from: the sum of the four 10-Gyr components; the sum of the three 1-Gyr components; the sum of two 100-Myr components; the sum of the two 10-Myr components; the sum of 3-Myr component and FC ($F_\nu \propto \nu^{-3/2}$). The top panel shows the internal reddening $E(B-V)_i$ obtained from the synthesis. At the bottom panel we also show the sum of the two metal-poor components (open dots, see the discussion in the text, Section 5.1). The vertical bars represent the standard deviation of the results. The vertical lines spanning the whole figure mark locations at 1 and 3 kpc from the nucleus.

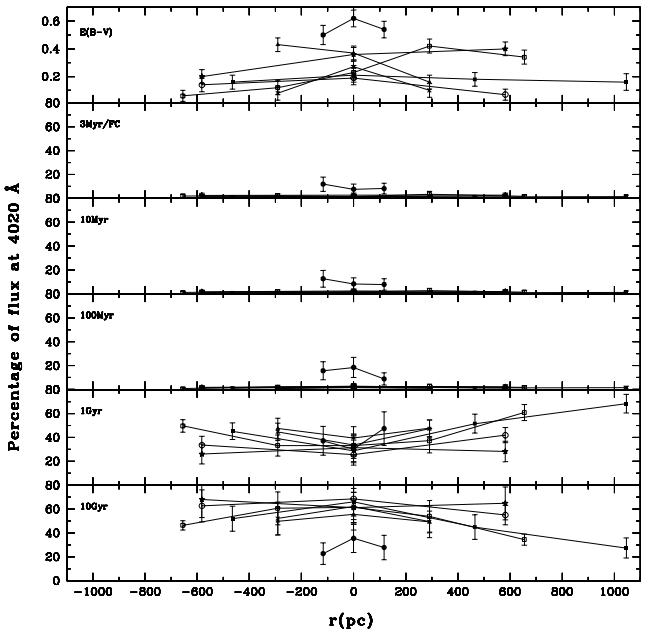

Figure 6. Results of stellar population synthesis for the non-Seyfert Sa–Sc galaxies plotted altogether. In order to group the results, we had first to transform the angular distances to linear distances at each galaxy. The galaxy with recent star formation is the Sc NGC 1637 (filled circle).

The results of the synthesis for the Sa–Sc non-Seyfert galaxies are summarized in Fig. 6, where we show the values for all non-Seyferts together, owing to the small number of points for each individual galaxy. In order to group the results, we had first to transform the angular distances to linear distances at each galaxy. For most galaxies, the stellar population in the nucleus is composed by ≈65 per cent of the 10-Gyr component and ≈30 per cent of the 1-Gyr component. The contribution of the other components are not significant. In six (of seven) galaxies the 10-Gyr component decreases while the 1-Gyr component increases outwards, similarly to the S0 non-Seyfert galaxy behaviour.

A distinct result is found for the Sc galaxy NGC 1637, which has recent star formation: at the nucleus the component of 10 Gyr contributes with 35 per cent, that of 1 Gyr with 30 per cent and those younger than 1 Gyr contribute the remaining 35 per cent of the flux at 4020 Å (we have little information on this galaxy concerning the stellar population outside the nucleus – only up to ≈100 pc from the nucleus).

The $E(B-V)_i$ values for these galaxies range from 0.1 to 0.6 and it is larger than those for S0 galaxies. The largest $E(B-V)_i$ is found for NGC 1637, the galaxy with recent star formation.

4.2 Synthesis results for the Seyfert 2 galaxies

In order to describe the synthesis results for the Seyfert 2 galaxies, we have grouped the sample into four classes according to their most important nuclear stellar component and describe the main characteristics (or variations) in the populations at the nucleus and outside, using the 1 and 3 kpc (when possible) locations as references. In the following discussion, we consider a population component significant when it contributes with at least 10 per cent of the total flux at 4020 Å.

4.2.1 Dominant 10-Gyr metal-rich stellar population

In this group are Mrk 573, NGC 5929, NGC 2110, Mrk 3, NGC 7212, Mrk 348 and Mrk 34, the nuclear stellar population of which is dominated by the 10-Gyr metal-rich (with solar or above metallicity) component. The galaxies are sorted above according the importance of the rich component, the contribution of which ranges from approximately 60 per cent of the total flux at 4020 Å in Mrk 573 to 30 per cent in Mrk 34. At the nucleus all of these galaxies have a contribution from the 1-Gyr component of at least 15 per cent of the total flux. Some of these objects also have significant nuclear contributions from younger components: Mrk 3 with 20 per cent of 3-Myr/FC, Mrk 34 with 10 per cent of 10 Myr old and 10 per cent of 3-Myr/FC and NGC 7212 with 15 per cent of 3-Myr/FC.

In Figs 7 and 8 we show the spatial variation of the spectral synthesis results for galaxies of this group. The extranuclear old metal-rich component contribution is similar to that of the nucleus in Mrk 3, Mrk 34 and NGC 2110, while in the other galaxies this component decreases outwards. The 1-Gyr component increases outwards in all galaxies. The younger components decrease outwards in the galaxies for which they are significant (>10 per cent) at the nucleus.

In Fig. 9 we compare the observed spectrum (solid line) with the synthetic one (dashed line) for one galaxy of this group (NGC 5929) at the nuclear and off-nuclear regions. The synthetic spectra were constructed using the star cluster templates (Bica & Alloin 1986, 1987) combined in the proportions given by the synthesis. The synthetic spectra reproduce the observed ones well, considering the lower spectral resolution of the available templates (≈10–20 Å) compared with the observations (≈3 Å).

4.2.2 Dominant 1-Gyr stellar population

The galaxies of this group are Mrk 78, NGC 1386, IC3639, Mrk 1073, NGC 1068, Mrk 1 and Mrk 1066, sorted according to the importance of the nuclear 1-Gyr component. In Mrk 78 this component contributes approximately 50 per cent of the total flux at 4020 Å and in Mrk 1066 with approximately 20 per cent. All of them have a significant nuclear contribution of the 10-Gyr component, and all except NGC 1386 also have a significant contribution from components younger than 1 Gyr.

The synthesis results as a function of distance from the nucleus for these galaxies are shown in Figs 10 and 11. Throughout the central 2 kpc the galaxies Mrk 78 and NGC 1386 have contributions of the 10-, 1-Gyr and 100-Myr components similar to those at the nucleus. NGC 1386 also has significant contributions from components 100 Myr old and younger outside the nucleus (at 300 and 660 pc), which is different from the nuclear one.

In Mrk 1066 the 10- and 1-Gyr components increase and those younger than 1 Gyr decrease outwards, while the population in IC3639 has the completely opposite behaviour.

The population outside the nucleus in Mrk 1 has contributions from the 1-Gyr and 100-Myr components similar to those at the nucleus and the contribution of the 10-Gyr component increases while that of the components younger than 100 Myr decreases. In Mrk 1073 the components of 10 and 1 Gyr have similar contributions to those at the nucleus and the contribution of the 100-Myr component increases while that of the components younger than 100 Myr decreases outwards.

In Fig. 12 we compare the observed spectrum (solid line) with the synthetic one (dashed line) for one galaxy of this group (Mrk 1073) at the nuclear and off-nuclear regions. All spectra present the high-order Balmer lines in absorption, characteristic of stellar populations younger than 1 Gyr.

4.2.2.1 NGC 1068. At the nucleus of this galaxy all components are significant but we would like to highlight the importance of the 3-Myr/FC component. It contributes approximately 17 per cent

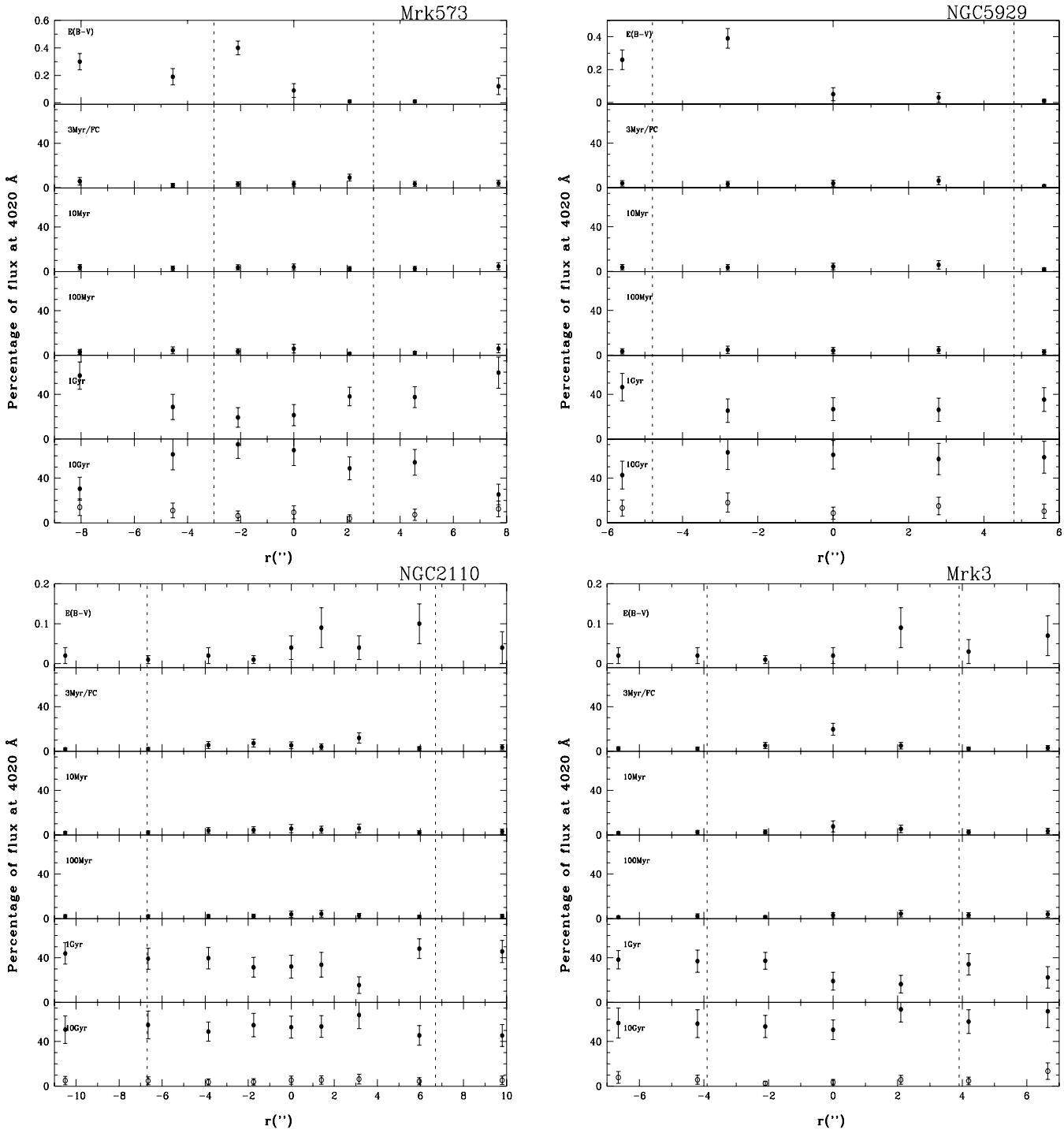

Figure 7. Results of stellar population synthesis as a function of the distance from the nucleus for the galaxies with a dominant 10-Gyr metal-rich component at the nucleus. The symbols are as in Fig. 5.

of the total light at 4020 Å. This result is consistent with the contribution of polarized light from the hidden Seyfert 1 nucleus (e.g. Antonucci et al. 1994).

Outside the nucleus, all age components continue to be important, contributing with more than 10 per cent to the flux at 4020 Å and indicating the presence of recent star formation throughout the observed region. In particular, at knot J (approximately 750 pc from the nucleus, NW – positive direction) and at knot C (approximately 2 kpc from the nucleus, SE – negative direction) the 3-Myr/FC component is as important as in the nucleus, contributing approximately 20 and 25 per cent, respectively. This result confirms that these are active star-forming regions. From the synthesis, knot C is younger than knot J. At 3 kpc from the nucleus the 3-Myr/FC component is not significant.

In Fig. 13 we compare the observed spectrum (solid line) with the synthetic one (dashed line) for the nucleus and knots C and J.

4.2.3 Dominant 100-Myr stellar population

In this group are Mrk 273, Mrk 533 and NGC 7130, for which the 100-Myr component contributes approximately 30 per cent to the

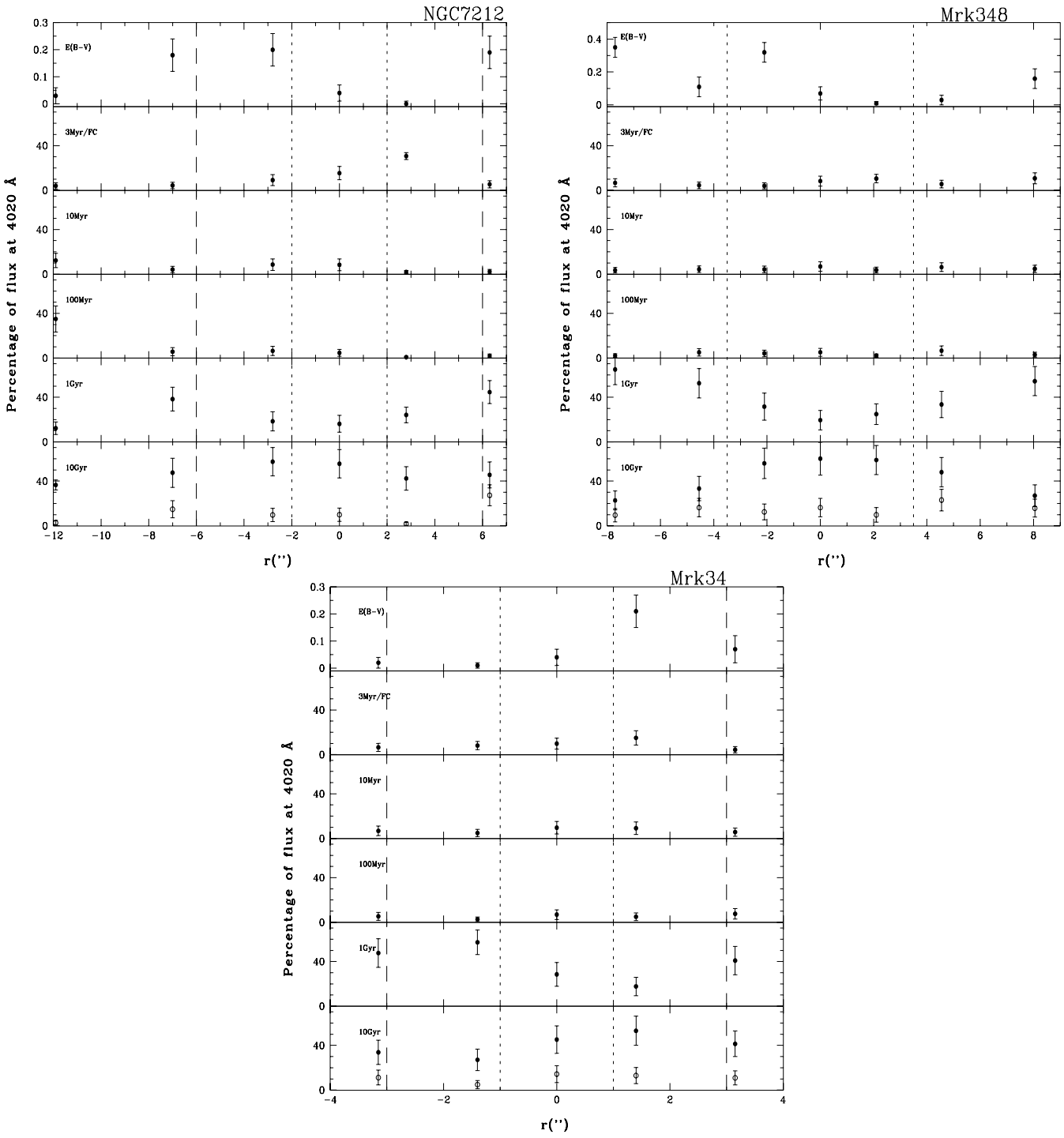

Figure 8. Synthesis results: galaxies with a dominant 10-Gyr metal-rich component at the nucleus.

nuclear flux at 4020 Å. The 10-Gyr component contributes approximately 20 per cent. The other components also have significant contributions at the nucleus of these galaxies, except 3-Myr/FC in Mrk 273.

The results of the synthesis for galaxies of this group are shown in Fig. 14. Outside the nucleus of NGC 7130 the contribution of 10- and 1-Gyr components increases while that of components younger than 100 Myr decreases.

The population of Mrk 533 shows large variations in the 10 Gyr, 100 and 3-Myr/FC components in the central 2 kpc. In the central 6 kpc the global tendencies are that the component with 1 Gyr increases and the 100-Myr component decreases outwards, while the 10-Gyr component and the components younger than 100 Myr have contributions similar to those at the nucleus.

In Mrk 273 the contributions do not vary significantly across the central 6 kpc.

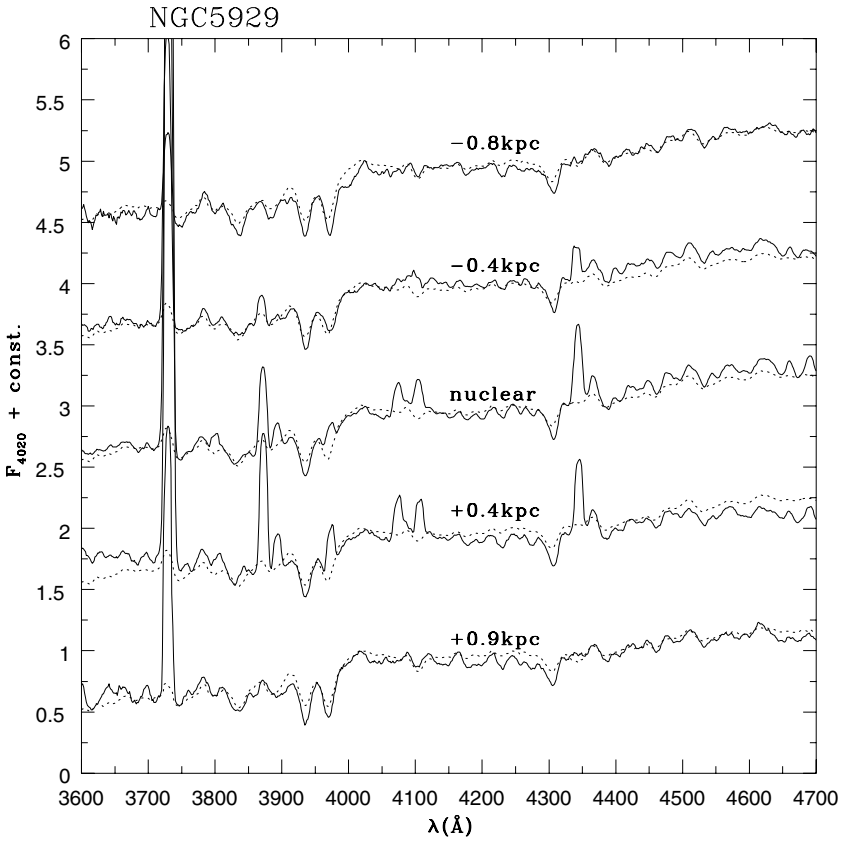

Figure 9. Observed and synthetic spectra at the nucleus and outside for one galaxy with a dominant 10-Gyr metal-rich component at the nucleus. The observed spectra were smoothed to match the lower resolution of the synthetic spectra.

In Fig. 15 we compare the observed spectrum (solid line) with the synthetic one (dashed line) for one galaxy of this group (Mrk 273) at the nuclear and off-nuclear regions. All spectra present the high-order Balmer lines in absorption, characteristic of stellar populations younger than 1 Gyr.

4.2.4 Dominant 3-Myr/FC component

Here are Mrk 463E, Mrk 477 and NGC 5135. The 3-Myr/FC component ranges from a 40 to a 30 per cent contribution to the nuclear flux at 4020 Å. Nuclei Mrk 463E and Mrk 477 also have significant flux contributions from the 10-, 1-Gyr and 10-Myr populations (approximately 15 per cent each). Besides those, the 100-Myr component contributes approximately 15 per cent at the nucleus of NGC 5135.

In Fig. 16 we show the synthesis results for these galaxies as a function of the distance from the nucleus. In Mrk 477 the contribution of the 3-Myr/FC component decreases and that of the 100-Myr component increases outwards. The other components have contributions similar to those at the nucleus.

Outside the nucleus of Mrk 463E the behaviour is not symmetric. At one side (positive direction) the 3-Myr/FC component decreases and the 10- and 100-Myr components increase outwards. At the other side these components have the opposite behaviour.

The stellar population of the galaxy Mrk 463E has been studied in R01 although with a different spatial sampling, spectral range for the observations and normalization wavelength for the synthesis. It is interesting to compare the results of the present work with those of R01 in order to verify the robustness of our method. This comparison shows a general agreement in the sense that the stellar population is dominated by the young components ($\leqslant$100 Myr old). Differences are found in the relative contribution of the 100- and 10-Myr components. Investigating the reason for this difference we conclude that it is caused by the fact that this galaxy has very small W values and the synthesis is strongly constrained by the continuum, which is affected by calibration uncertainties. Nevertheless, within the scope of the present paper, these differences do not alter our main conclusions.

In NGC 5135 the contribution of the 10- and 1-Gyr components increases and that of the components younger than 1 Gyr decreases outwards.

In Fig. 17 we compare the observed spectrum (solid line) with the synthetic one (dashed line) for one galaxy of this group (Mrk 477) at the nuclear and off-nuclear regions. The nuclear spectrum is dominated by gas emission of the AGN narrow-line region and the star-forming regions. Outside the emission decreases and we can see the high-order Balmer lines in absorption, characteristic of stellar populations younger than 1 Gyr.

We summarize the synthesis results discussed above in Table 4 which shows the contribution of four age bins: 10, 1 Gyr, 100 + 10 Myr and 3-Myr/FC to the nuclear and extranuclear spectra (at 1 and 3 kpc from the nucleus) of the sample. The Seyfert 2 galaxies are grouped according to the Hubble type (from top to bottom) in the top part of table: the first group contains the S0 galaxies, the second the Sa–Sbs, the third the Sbcs and the fourth the galaxies with an uncertain morphological type. In the bottom part of the table are those for the non-Seyfert galaxies. For these galaxies, owing to the smaller signal-to-noise ratio of the 1.5-m observations, we could only reach distances at the galaxies somewhat smaller than 1 kpc. In order to allow a comparison with the Seyfert data we

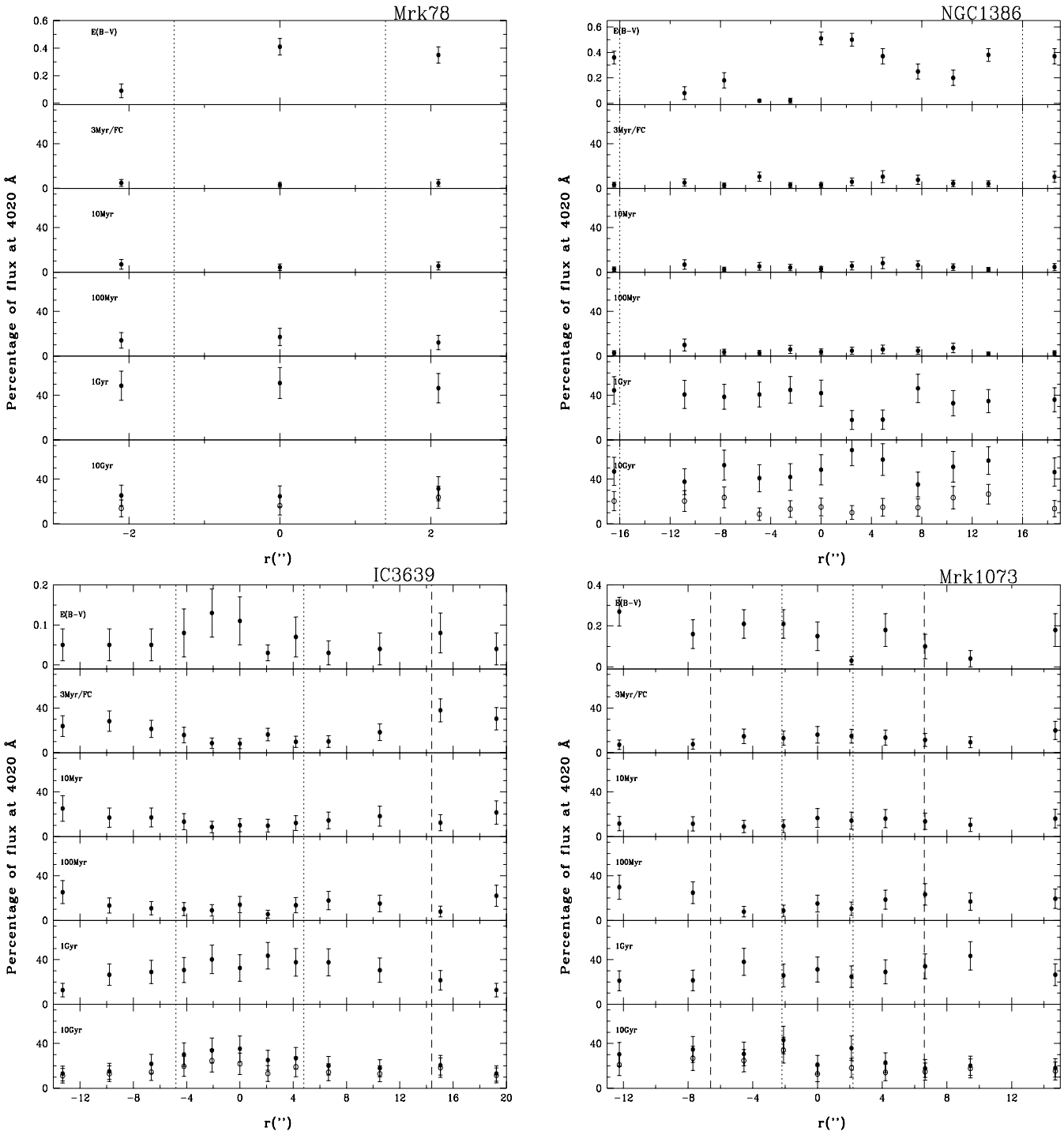

Figure 10. Synthesis results: galaxies with a dominant 1-Gyr component at the nucleus.

decided to show the results for the synthesis at 1 kpc from the nucleus, obtained by extrapolation from the extranuclear spectra. We performed the extrapolation based on the hypothesis that the stellar population varies smoothly with the distance from the nucleus, such as in the S0 non-Seyfert galaxies studied in R01. This seems to be a reasonable assumption, if one compares Fig. 5 with Fig. 6, which show similar behaviour of the stellar population gradients for the S0 and later Hubble types. The extrapolated values are shown between parentheses in Table 4.

$E(B-V)_i$ values are found throughout the observed region in the range $0 < E(B-V)_i < 0.7$. The large $E(B-V)_i$ variations present in almost all Seyfert 2 galaxies are likely to be caused by a non-uniform dust distribution (Malkan et al. 1998).

5 DISCUSSION

From the synthesis results, the main characteristics of the stellar population of the present Seyfert 2 sample are as follows.

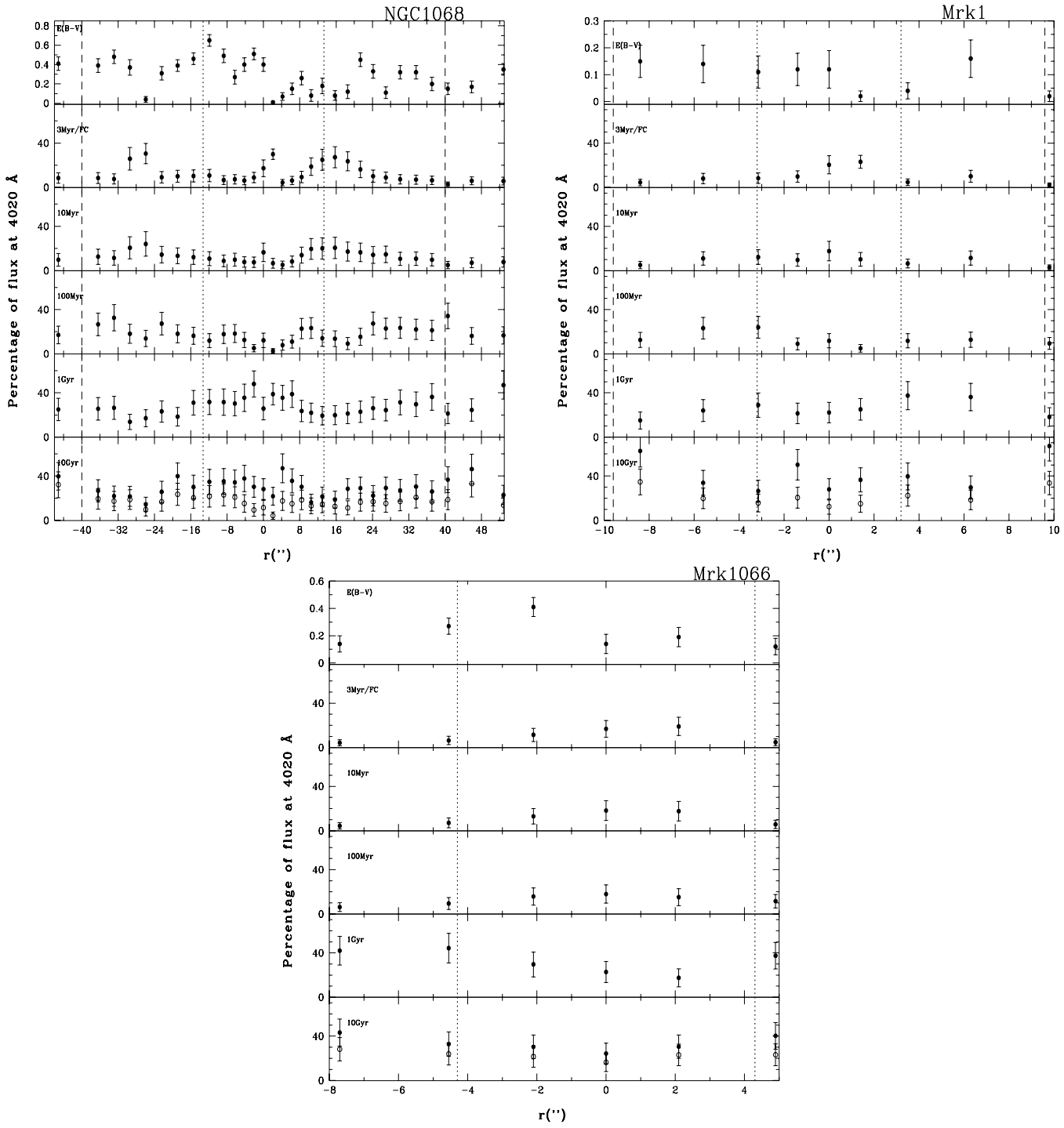

Figure 11. Synthesis results: galaxies with a dominant 1-Gyr component at the nucleus.

(i) At the nucleus 75 per cent of the sample (15 galaxies) have a contribution of ages $\leqslant$100 Myr (or/and FC) larger than 20 per cent. This result is in agreement with those of Schmitt et al. (1999), Storchi-Bergmann et al. (2000) and González Delgado et al. (2001), who found that in $\approx$40 per cent of nearby Seyfert 2 galaxies there are clear signatures of young stars and in another 30 per cent there is a blue continuum that can be either a result of an FC or a stellar population younger than 10 Myr. 55 per cent (11 galaxies), have a significant (>10 per cent) 3-Myr/FC component at the nucleus.

(ii) At 1 kpc from the nucleus, 70 per cent of the sample has a contribution of ages $\leqslant$100 Myr (or/and FC) larger than 20 and 50 per cent have a significant 3-Myr/FC component.

(iii) At 3 kpc, 45 per cent of the sample has a contribution of ages $\leqslant$100 Myr (or/and FC) larger than 20 and 25 per cent have a significant 3-Myr/FC population.

(iv) The contribution of the 1-Gyr component increases outwards from the nucleus in 13 galaxies while the old metal-rich component decreases in seven galaxies. This behaviour was also found in S0 non-Seyfert galaxies studied by R01.

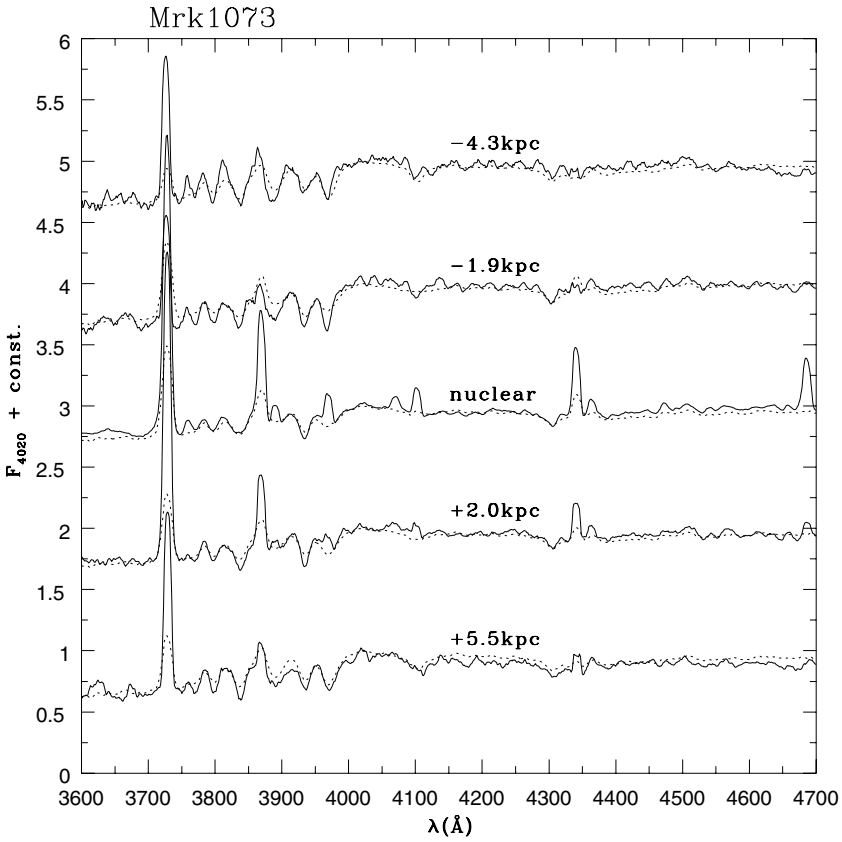

Figure 12. As in Fig. 9 for one galaxy with a dominant 1-Gyr component at the nucleus.

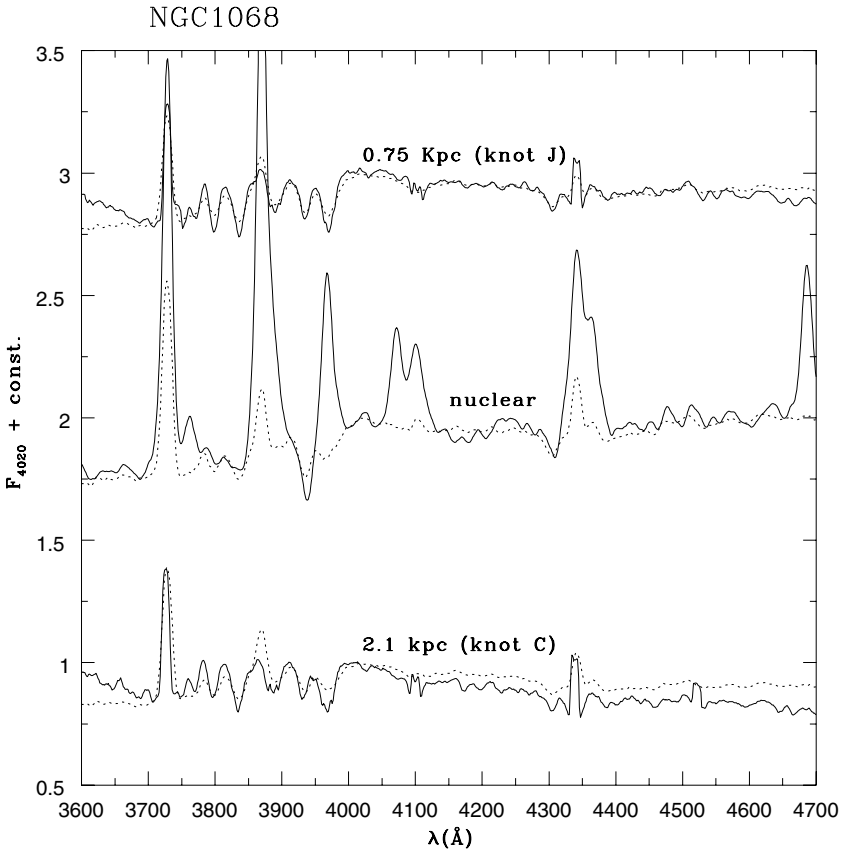

Figure 13. As in Fig. 9 for NGC 1068 and two knots of star formation.

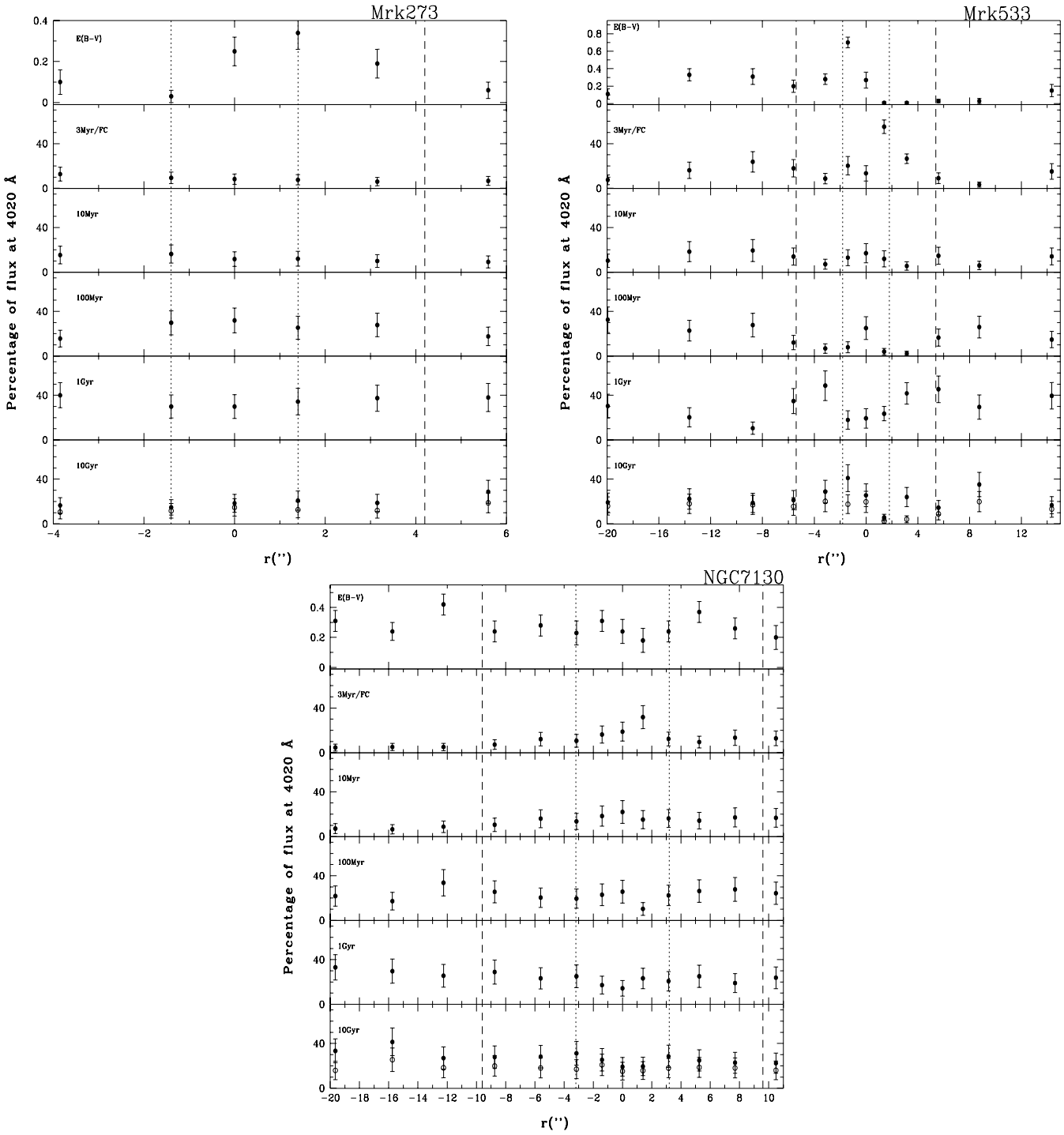

Figure 14. Synthesis results: galaxies with a dominant 100-Myr component at the nucleus.

(v) The contribution of the old metal-poor component is significant in 17 galaxies of the sample.

The latter result was also found in R01 and in that work we hypothesized that this contribution (larger than that found in non-Seyfert S0 galaxies) could be an effect of degeneracy between the old metal-poor component and the 3-Myr/FC component. In order to verify whether this effect is important we repeated the spectral synthesis excluding the metal-poor components. In Fig. 18 we show the results of the synthesis without these components (crosses) as compared with the synthesis using all components (filled dots), for two extreme cases: Mrk 348 and IC3639.

In Mrk 348, in the new synthesis, the missing contribution of the metal-poor components is shared among all other younger components and the only significant change is in the 10-Gyr population, which decreases to approximately 15 per cent of the total flux at 4020 Å. In the other extreme case of IC3639, while the old population decreases by approximately 20 per cent, the 100-Myr

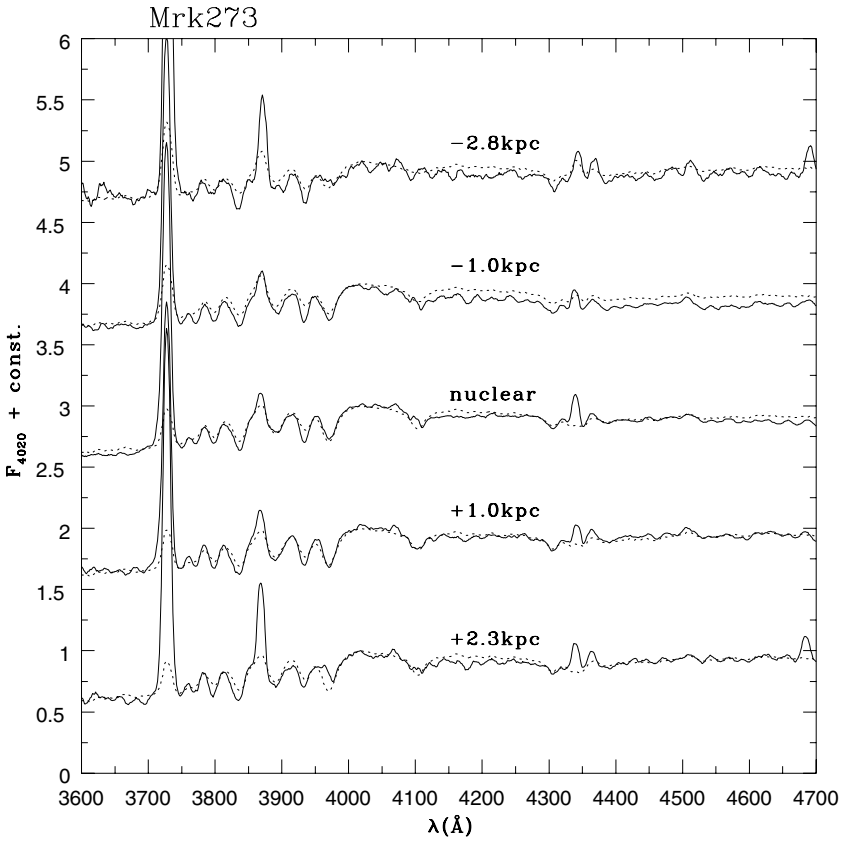

Figure 15. As in Fig. 9 for one galaxy with a dominant 100-Myr component at the nucleus.

component increases by approximately 10 per cent in the new synthesis. The remaining 10 per cent is shared among the other components.

We thus conclude that such possible degeneracy effects are not large in the synthesis. In addition, although the 10-Gyr metal-poor component presents a small contribution in S0s, B88 shows that this component is larger in later-type galaxies, and we would thus need to compare the results for the Seyferts with those of non-Seyfert galaxies of the same Hubble type, considering that, besides seven S0/Sas, the present sample comprises four Sab/Sbs and two Sbcs, and seven galaxies with uncertain morphology.

5.1 Comparison with synthesis results for non-active galaxies

A comparison of the Seyfert 2 stellar population properties and their radial variations with those of non-active galaxies of the same Hubble type is necessary in order to search for systematic differences in the Seyfert sample, which could be related to the AGN phenomenon.

In Table 4 we summarize the individual synthesis results for the Seyfert 2 and non-Seyfert galaxies and in Table 5 we show the corresponding average results for each Hubble type, also including those for the three non-Seyfert S0 galaxies from R01 and the reference sample of B88 (in this latter case we show the integrated results from apertures of $\approx 1 \times 1$ kpc).

Presently, we have three S0 non-Seyfert galaxies studied with the same method applied to the present Seyfert 2 sample, large spatial coverage (up to 3 kpc from the nucleus) and typical sampling regions at the galaxy of 200 pc. For Hubble types later than S0, we have the seven non-Seyfert galaxies studied in this work, with a more restricted spatial coverage and a similar typical sampling. In order to compare the results for these Sa–Sc galaxies with those for the active ones, we had to extrapolate the stellar population synthesis to 1 kpc using the nuclear and available extranuclear spectra.

Because the number of non-Seyfert galaxies is reduced we also use as a reference the study of B88. We have performed the spectral synthesis of the templates using the same *W*s and *C*s used for our sample. The synthesis results were then averaged in order to obtain the 'typical' population of each Hubble-type Sa, Sb and Sc. As the dimensions of the regions studied by B88 are much larger than those corresponding to our nuclear extractions, we need to take into account both the nuclear and extranuclear synthesis results from our Seyfert 2 sample in the comparison with the non-Seyfert galaxies.

Comparing the synthesis results for the Seyferts with those for non-Seyferts of the same Hubble type we realize that, at the nucleus, the contribution of the 10-Gyr component is smaller in Seyfert 2 galaxies than in non-Seyfert galaxies in 11 (of the 13, which have Hubble types from S0 to Sbc) of them. The component with 1 Gyr is similar in Seyfert 2 and non-Seyfert galaxies in four objects, larger in five Sy2 and smaller in four. In terms of average values (for each Hubble type) the 1-Gyr contribution is larger for S0 Sy2, and comparable to that of non-Seyferts for Sa to Sbc Hubble type. The components younger than 1 Gyr and FC are larger in Sy2 than in non-Seyferts in 11 galaxies.

At 1 kpc from the nucleus we found for S0 galaxies that the contribution of the 10-Gyr component is always smaller in Sy2 than in non-Seyferts, while the contribution of the 1-Gyr and younger components are normally larger. In the later Hubble-type galaxies we usually have a smaller contribution of both the 10- and 1-Gyr

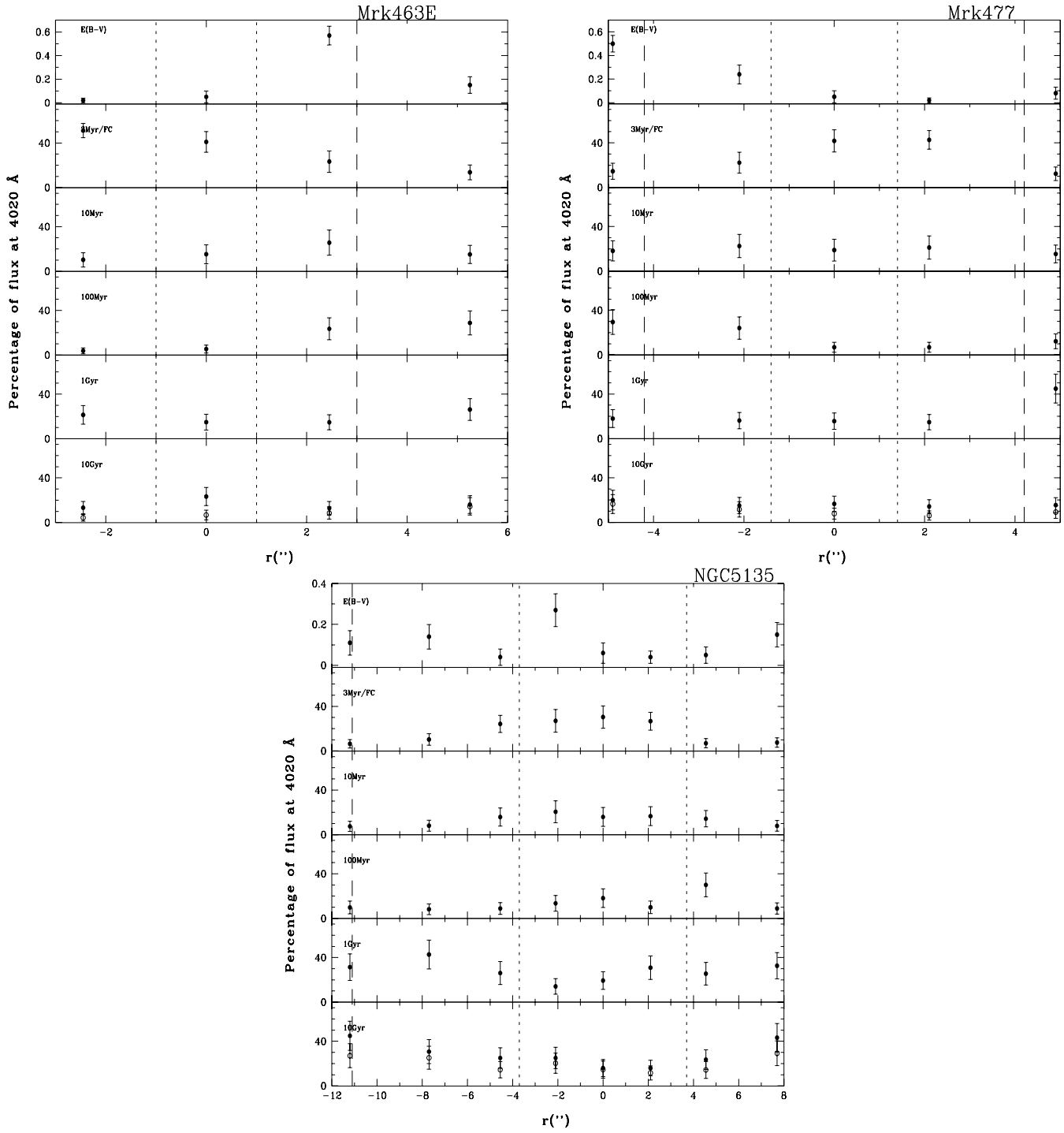

Figure 16. Synthesis results: galaxies with a dominant 3-Myr/FC component at the nucleus.

components and a larger contribution of the youngest components in Sy2s than in non-Seyferts.

There are seven galaxies with uncertain morphology: Mrk 1, Mrk 34, Mrk 78, Mrk 273, Mrk 463E, Mrk 477 and NGC 7212, all but Mrk 34 and Mrk 78 in clear interaction. At the nucleus all of them have a significant contribution of components younger than 1 Gyr, while at 3 kpc from the nucleus only for two of them does this not happen. We do not have a reference study, similar to that we have performed here, for the stellar population in non-active interacting galaxies, but it is a well-known result that these galaxies frequently show recent episodes of star formation, triggered by the interaction (Sanders & Mirabel 1996 and references therein). Thus the results we have obtained for these Seyfert 2 galaxies do not seem peculiar.

Regarding the $E(B-V)_i$ values, non-Seyferts S0 galaxies present a small internal reddening throughout the central 6 kpc while Seyfert galaxies of the same Hubble type normally have larger values and a large variation. For later-type galaxies, we did not find significant differences between Seyfert and non-Seyfert galaxies.

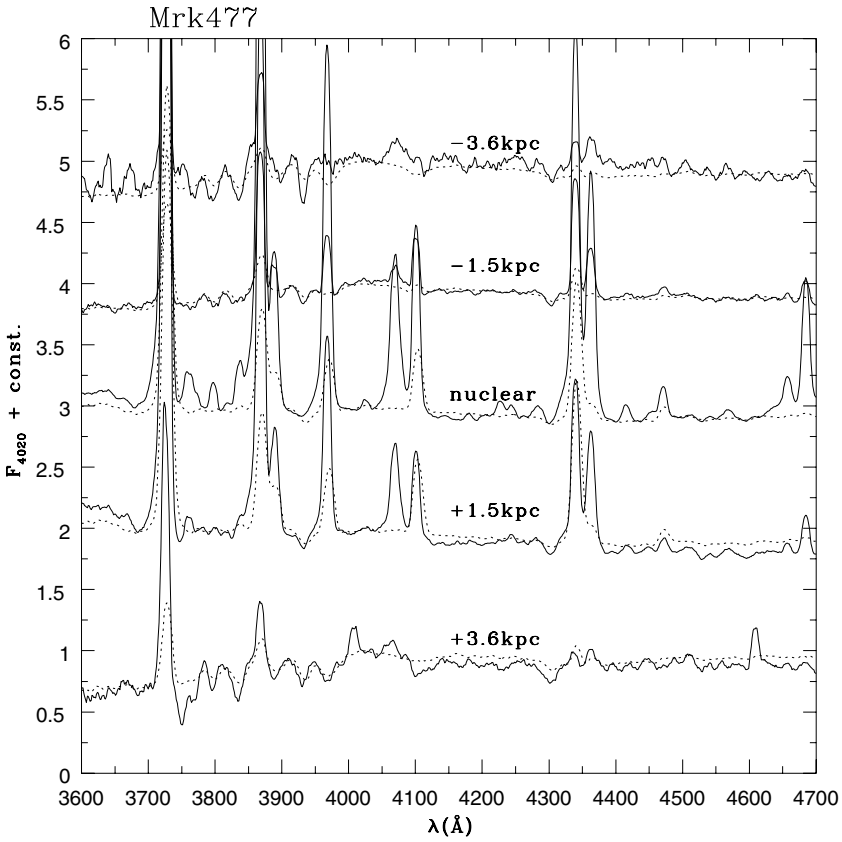

Figure 17. As in Fig. 9 for one galaxy with a dominant 3-Myr/FC component at the nucleus.

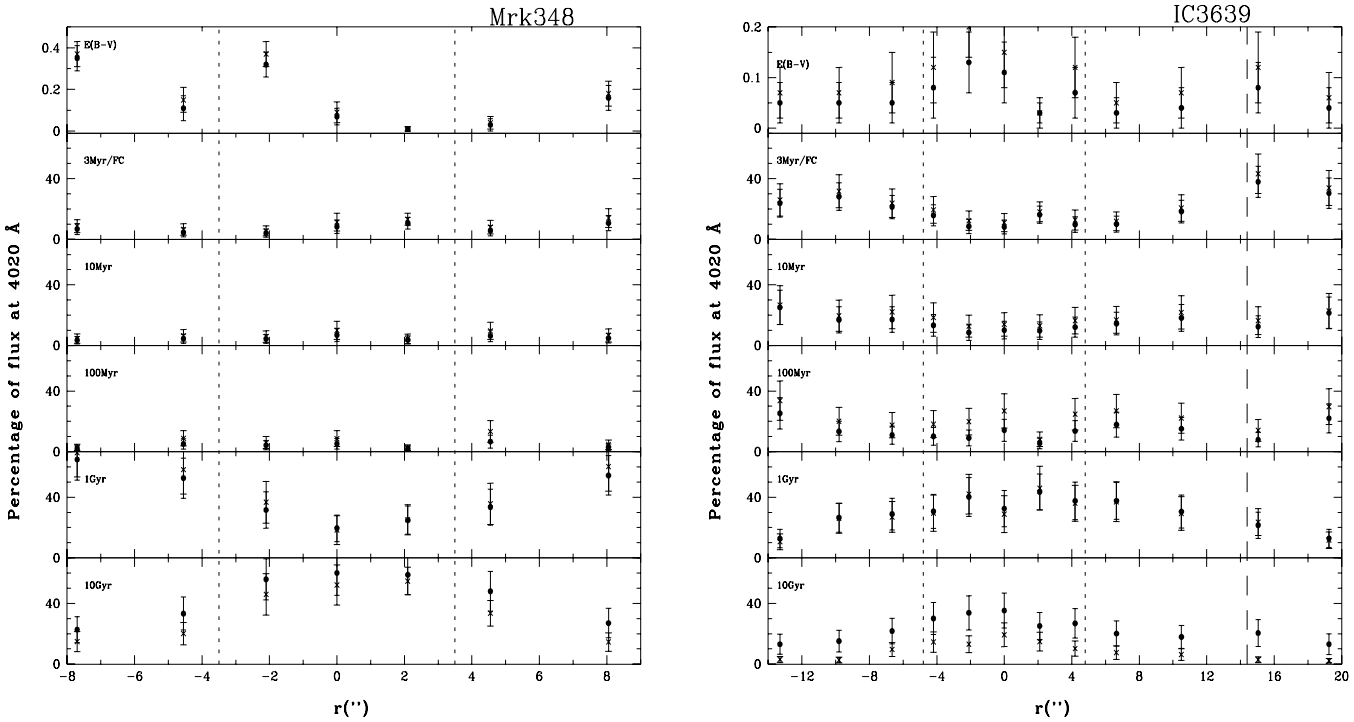

Figure 18. Results of the synthesis performed with all base components (filled dots) and without the metal-poor components of 10 and 1 Gyr (crosses) for two cases (see the discussion in Section 5). Panels as in Fig. 5.

Table 4. Contribution of four age bins to the total flux at 4020 Å, for the sample galaxies. In the first group (top) are the S0 Sy2 galaxies, in the second the Sa–Sb Sy2s, in the third the Sbc Sy2s and in the fourth the galaxies with uncertain morphological type. In the second part of the table are the non-Seyfert galaxies grouped by morphological type. The numbers on parentheses were extrapolated from the extranuclear spectra.

Name	10 Gyr			1 Gyr			100+10 Myr			3-Myr/FC		
	Nuclear	1 kpc	3 kpc	Nuclear	1 kpc	3 kpc	Nuclear	1 kpc	3 kpc	Nuclear	1 kpc	3 kpc
S0 Seyfert 2												
Mrk 3	50	56	–	20	37	–	10	5	–	20	2	–
Mrk 348	60	49	–	20	35	–	12	10	–	8	6	–
Mrk 573	65	60	–	21	29	–	10	7	–	4	4	–
Mrk 1066	24	33	–	23	40	–	36	17	–	17	6	–
NGC 1386	48	50	–	42	38	–	7	4	–	3	8	–
NGC 2110	53	50	–	32	43	–	10	4	–	5	3	–
Sa–Sb Seyfert 2												
Mrk 1073	21	39	26	31	25	30	32	22	36	16	14	8
NGC 1068	29	25	43	26	26	26	28	31	24	17	18	7
NGC 5135	16	24	45	20	29	31	34	31	18	30	16	6
NGC 5929	61	53	–	27	34	–	8	9	–	4	4	–
NGC 7130	19	29	25	14	23	26	48	36	38	19	12	11
Sbc Seyfert 2												
Mrk 533	26	23	18	19	22	40	41	18	28	14	37	14
IC3639	36	26	17	31	30	23	24	30	36	9	14	24
S Seyfert 2												
Mrk 1	28	33	64	22	34	17	30	27	15	20	6	4
Mrk 34	45	40	37	29	37	45	16	12	12	10	11	6
Mrk 78	24	27	–	51	48	–	21	20	–	4	5	–
Mrk 273	19	18	23	29	33	38	44	41	32	8	8	7
Mrk 463E	24	19	15	15	17	20	20	28	46	41	36	19
Mrk 477	17	15	18	16	16	29	26	36	36	41	33	17
NGC 7212	57	55	48	16	18	40	12	9	8	15	18	4
Non-Seyfert Sa–Sb												
NGC 1367	61	(40)	–	33	(55)	–	4	(4)	–	2	(1)	–
NGC 1425	62	(25)	–	34	(75)	–	3	(0)	–	1	(0)	–
NGC 3358	61	(70)	–	31	(25)	–	5	(3)	–	3	(2)	–
Non-Seyfert Sbc												
NGC 3054	66	(30)	–	29	(70)	–	3	(0)	–	2	(0)	–
NGC 3223	69	(55)	–	26	(45)	–	4	(0)	–	1	(0)	–
Non-Seyfert Sc												
NGC 1232	56	(38)	–	40	(62)	–	4	(0)	–	1	(0)	–
NGC 1637	35	–	–	30	–	–	27	–	–	8	–	–

Both present large $E(B-V)_i$ variations (from 0 to 0.7), probably caused by a non-uniform dust distribution.

6 SUMMARY AND CONCLUSIONS

In this paper we have analysed the stellar population of a sample of 20 Seyfert 2 galaxies as a function of the distance from the nucleus, comparing the contribution of different age components with those for non-Seyfert galaxies of the same Hubble type.

The main conclusions can be summarized as follows.

(i) The radial distribution of the Ca II *K* and *G* band *W*s show smaller values at the nucleus than that at ≈1 kpc from it for 11 of the 20 Seyfert 2 galaxies of the sample, suggesting dilution by a blue continuum from an FC or young stars; two present larger *W* values at the nucleus than outside, similar to non-Seyfert S0 galaxies, and in the remainder there is no obvious dilution, nor a systematic variation with the distance similar to that observed for the S0 galaxy.

(ii) A stellar population synthesis shows that, while at the nucleus, 75 per cent of the galaxies present a contribution ⩾20 per cent of ages ⩽100 Myr (or/and FC), this proportion decreases to 45 per cent at 3 kpc. In particular, 55 per cent of the galaxies have a contribution >10 per cent of the 3-Myr/FC component at the nucleus, but only 25 per cent of them having this component at 3 kpc.

(iii) Our results point to a systematic difference between the stellar population of Seyfert galaxies and those of non-Seyfert galaxies for the Hubble types from S0 to Sbc. At the nucleus and up to 1 kpc from it the contribution of ages younger than 1 Gyr is in most cases larger in the Seyferts than in non-Seyfert galaxies. Regarding the 1-Gyr component, at the nucleus its contribution is for the Seyferts, on average, larger for S0s and similar to that of non-Seyfert for later-type galaxies. Outside the nucleus it is again larger for the S0 Sy2s but smaller for the later type Seyfert when compared with the non-Seyferts. The 10-Gyr component shows a larger contribution in non-Seyferts than in Seyferts. Both the Seyferts and non-Seyferts show a decrease of the contribution of the 10-Gyr component and an increase of the 1-Gyr component with distance from the nucleus, although the gradient seems to be steeper for the non-Seyfert galaxies.

In the evolutionary scenario proposed by Storchi-Bergmann et al. (2001) and Cid Fernandes et al. (2001), the results above indicate that the interactions that trigger the AGN and circumnuclear bursts

Table 5. Average contribution of four age bins to the total flux at 4020 Å, for different Hubble types. The numbers on parenthesis were extrapolated from the extranuclear spectra.

Hubble type	10 Gyr			1 Gyr			100+10 Myr			3-Myr/FC		
	Nuclear	1 kpc	3 kpc	Nuclear	1 kpc	3 kpc	Nuclear	1 kpc	3 kpc	Nuclear	1 kpc	3 kpc
S0 Seyfert 2	50	50	–	26	37	–	14	8	–	10	5	–
Non-Seyfert S0	86	77	50	6	15	36	9	8	12	0	0	1
Sa–Sb Seyfert 2	29	34	35	24	27	28	30	26	29	17	13	8
Non-Seyfert Sa–Sb	61	(45)	–	33	(52)	–	4	(2)	–	2	(1)	–
Bica' Sa[a]	56	–	–	37	–	–	4	–	–	2	–	–
Bica' Sb[a]	53	–	–	35	–	–	7	–	–	5	–	–
Sbc Seyfert 2	31	25	17	25	26	32	33	24	32	12	26	19
Non-Seyfert Sbc	68	(43)	–	27	(57)	–	3	(0)	–	2	(0)	–
Non-Seyfert Sc	46	–	–	35	–	–	15	–	–	4	–	–
Bica' Sc[a]	27	–	–	27	–	–	26	–	–	20	–	–
S Seyfert 2	31	30	34	25	29	32	24	24	24	20	16	10

[a]Results for non-Seyfert galaxies from Bica (1988), in a region of 1×1 kpc^2.

of star formation, also trigger bursts along the body of the galaxy, at least within the inner 1 kpc.

ACKNOWLEDGMENTS

DR, TSB and RCF acknowledge support from the Brazilian Institutions CNPq, CAPES and FAPERGS. The National Radio Astronomy Observatory is a facility of the National Science Foundation operated under cooperative agreement by Associated Universities, Inc. We thank an anonymous referee for valuable suggestions that helped to improve the paper.

REFERENCES

Antonucci R., 1993, ARA&A, 31, 473
Antonucci R., Hurt T., Miller J., 1994, ApJ, 430, 210
Aretxaga I., Terlevich E., Terlevich R.J., Cotter G., Díaz Á.I., 2001, MNRAS, 325, 63
Bica E., 1988, A&A, 195, 76 (B88)
Bica E., Alloin D., 1986, A&A, 162, 21
Bica E., Alloin D., 1987, A&A, 186, 49
Canalizo G., Stockton A., 2001, ApJ, 555, 719
Cid Fernandes R., Terlevich R., 1995, MNRAS, 272, 423
Cid Fernandes R., Jr, Storchi-Bergmann T., Schmitt H.R., 1998, MNRAS, 297, 579
Cid Fernandes R., Sodré L., Schmitt H., Leão J.R., 2001a, MNRAS, 325, 60
Cid Fernandes R., Heckman T., Schmitt H., González Delgado R.M., Storchi-Bergmann T., 2001b, ApJ, 558, 81
González Delgado R., Heckman T.M., Leitherer C., Meurer G.R., Krolik J., Wilson A.S., Kinney A., Koratkar A., 1998, ApJ, 505, 174
González Delgado R., Heckman T.M., Leitherer C., 2001, ApJ, 546, 845
Heckman T.M. et al., 1995, ApJ, 452, 549
Heckman T.M., González Delgado R., Leitherer C., Meurer G.R., Krolik J., Kinney A., Koratkar A., Wilson A.S., 1997, ApJ, 482, 114
Joguet B., Kunth D., Melnick J., Terlevich R., Terlevich E., 2001, A&A, 380, 19
Malkan M.A., Gorjian V., Tam R., 1998, ApJSS, 117, 25
Neff S.G., Fanelli M.N., Roberts L.J., O'Connell R.W., Bohlin R., Roberts M.S., Smith A.M., Stecher T.P., 1994, ApJ, 430, 545
Oliva E., Origlia L., Maiolino R., Moorwood A.F.M., 1999, A&A, 350, 90
Raimann D., Storchi-Bergmann T., Bica E., Alloin D., 2001, MNRAS, 324, 1087 (R01)
Sanders D.B., Mirabel F.I., 1996, ARA&A, 34, 749
Schmitt H.R., Storchi-Bergmann T., Cid Fernandes R., 1999, MNRAS, 303, 173
Storchi-Bergmann T., Cid Fernandes R., Schmitt H.R., 1998, ApJ, 501, 94
Storchi-Bergmann T., Raimann D., Bica E., Fraquelli H., 2000, ApJ, 544, 747
Storchi-Bergmann T., González Delgado R., Schmitt H.R., Cid Fernandes R., Heckman T., 2001, ApJ, 559, 147
Tadhunter C., Dickson R., Morganti R., Robinson T.G., Wills K., Villar-Martin M., Hughes M., 2002, MNRAS, 330, 977
Whittle M., 1992a, ApJ, 387, 121
Whittle M., 1992b, ApJS, 79, 49

This paper has been typeset from a TEX/LATEX file prepared by the author.